


Field trip guide to the Mineral Deposits of Poland, 16 June - 25 June 2018

SEG Student Chapter ETH Zürich

Report**Author(s):**

Arnold, Jeremias; Bernard, Cyrielle; Castellanos-Meléndez, Maria Paula; Zabihian, Farid; Fiedrich, Alina; Logan, Leslie; Reyes Alvarez, Julian Mauricio; Roodpeyma, Taraneh; Schirra, Michael; [Sliwinski, Jakub](#) ; Solms, Thierry

Publication date:

2018-06-12

Permanent link:

<https://doi.org/10.3929/ethz-b-000269095>

Rights / license:

In Copyright - Non-Commercial Use Permitted

ETH zürich



Field trip guide to the **Mineral Deposits of Poland**

16 June -25 June 2018



Edited by Alina Fiedrich, Michael Schirra, and Leslie Logan
Institute of Geochemistry and Petrology, ETH Zurich

Photo of Rudna mine from <http://kghm.com/en/our-business/mining-and-enrichment/rudna>
(retrieved on 24.05.2018)

Field trip guide to the Mineral Deposits of Poland



Contributions

The contributions to the field guide were compiled from the literature by the students of the society of economic geologists (SEG) student chapter of ETH Zurich, who take responsibility for correct referencing of data sources, to the best of their knowledge. There is no own research beyond the literature study involved.

Support

We gratefully acknowledge the financial support by the Institute of Geochemistry and Petrology of ETH Zurich and Pan American Silver, and we appreciate the logistical and scientific support by the SGA Baltic student chapter at AGH Kraków and the Institute of Geological Sciences at University of Wrocław.

Published in the ETH Research Collection, June 2018, © ETHZ 2018

ISBN: 978-3-906916-25-5
DOI: 10.3929/ethz-b-000269095

Table of Contents

Participants.....	3
General Information.....	4
Field trip program.....	5
Itinerary.....	8
Geology of Poland.....	10
The Wieliczka salt mine.....	13
The Szklary gemstone mine.....	16
The Lower Silesian Chromitites.....	19
The Kupferschiefer Deposits of Poland.....	23
The Bełchatów open pit coal mine: geology, current state and future of lignite mining in Poland.....	28
Carbonate-hosted Pb-Zn deposits in the Upper Silesia: geological setting and ore precipitation mechanisms.....	32
Pomorzany-Olkusz mines and the Silesia-Cracow District: fluid inclusions and insight into ore deposition processes.....	34
The Piast-Ziemowit hard coal mine, underground techniques.....	38
The Tarnowskie Góry mining museum.....	41
Appendix: International Chronostratigraphic Chart.....	46

Participants

Students

Arnold, Jeremias	BSc student, ETHZ	jarnold@student.ethz.ch
Bernard, Cyrielle	PhD student, GET-OMP	cyrielle.bernard@get.omp.eu
Bulcewicz, Kamil	University of Wrocław	kamil.bulcewicz@gmail.com
Castellanos Melendez, Maria Paula ²	MSc student, ETHZ	casmaria@student.ethz.ch
Farid Zabihian	associate	faridzabihian69@gmail.com
Fiedrich, Alina ¹	PhD student, ETHZ	alina.fiedrich@erdw.ethz.ch
Ligeza, Gabriela ³	MSc student, ETHZ	gligeza@student.ethz.ch
Logan, Leslie ^{1,2}	MSc student, ETHZ	llogan@student.ethz.ch
Nowak, Małgorzata	University of Wrocław	
Reyes Alvarez, Julian Mauricio ¹	MSc student, ETHZ	rejulian@student.ethz.ch
Roodpeyma, Taraneh	PhD student, ETHZ	t_roodpeyma@yahoo.com
Schirra, Michael ¹	PhD student, ETHZ	michael.schirra@erdw.ethz.ch
Sliwinski, Jakub ²	PhD student, ETHZ	jakub.sliwinski@erdw.ethz.ch
Solms, Thierry	MSc student, ETHZ	tsolms@student.ethz.ch
Szkrynecki, Jakub ³	PhD student, University of Leeds	jakubskrynecki@gmail.com

¹ Organizers, ² Drivers, ³ Guests

Contacts in Poland

Tomasz Cwiertnia and Wladyslaw Zygo
SGA Baltic student chapter
AGH University of Science and Technology, Kraków
Department of Ore Deposits and Mining
Al. Mickiewicza 30
tcwiertnia@geol.agh.edu.pl
wzygo@geol.agh.edu.pl
+48 12 617 24 47

Dr. Wojciech Śliwiński
Institute of Geological Sciences
University of Wrocław
ul. Cybulskiego 30
wojciech.sliwinski@uwr.edu.pl
+48 605 676 453

Dr. Piotr Wojtulek
Institute of Geological Sciences
Department of Economic Geology
University of Wrocław
pl. Maxa Borny 9
piotr.wojtulek@uwr.edu.pl
+48 71 375 94 36

General Information

Important dates:

- 07.05.2018 - Pre-excursion logistics meeting
- 11.07.2018 - Pre-excursion seminar with 10 min presentations
- 15.06.2018 - Departure from Zurich HB

Do not forget:

- field guide
- passport (or ID card for EU-EFTA citizens)
- Ausländerausweis
- student card (Legi) - important for museums
- driver's license (European or Swiss)
- credit card or cash (Złoty) for personal purchases
- info about health & accident insurance in case of emergency

- solid shoes (e.g. hiking boots)
- field clothes (long sleeves, nothing fancy)
- rain gear
- sunscreen, mosquito spray
- towel (for hostels and mines)
- sneakers or flip-flops (for hostels, city tours)

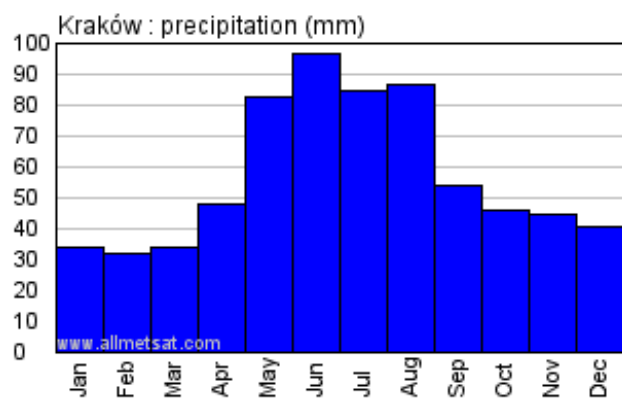
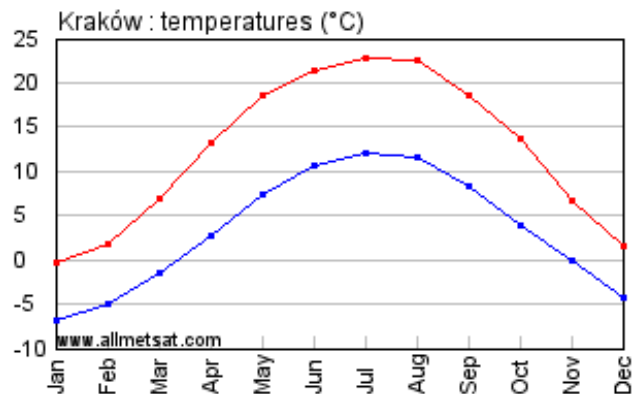
Be prepared for both warm and cold, rainy weather. Clothes will get dirty during mine visits. There won't be any opportunity to do laundry, so bring enough for the ten days but avoid unnecessary baggage.

- field note book & pencils
- camera
- hammer, pocket knife, magnet, etc.
- sampling bags, sharpie
- water bottle
- snacks for the train ride, small breakfast
- small present for the people who will guide and help us during the field trip

Driving in Poland

Wear seat belts at all times, do not use cell phones while driving, turn on the lights (also during the day), drive on the right side, give way to trams and buses, do not drink alcohol, and watch out for pedestrians on the road.

Climate in Silesia



Some Polish expressions

- Good Morning! - Dzień dobry!
- Thanks! - Dziękuję!
- yes - tak
- no - nie
- Help! - Pomocy!
- I don't speak Polish. - Niestety nie mówię po polsku.
- Where's the toilet? - Gdzie znajduje się toaleta?
- I'm lost. - Zgubiłem / Zgubiłam się.

In case of emergency:

- 999 - ambulance
- 997 - police
- 998 - fire brigade
- 981 - road assistance

Field trip program

15.06.2018 - Departure from Zurich HB

All participants except guests and Cyrielle meet at the platform at Zurich main station 15 min before departure. Train tickets cannot be handed out in advance, as we will travel as a group.

Connection:

15.06. Zurich to Vienna, NJ467 (couchette)
21:40 - 07:55

16.06. Vienna to Katowice, EC104 (seats)
8:10 - 12:33

16.06.2018 - Meeting with students in Kraków

After having arrived in Katowice, the two rental cars will be picked up at Katowice main station and Katowice airport by Leslie and Jakub, respectively. Cyrielle will be picked up at the rental car agency at Katowice airport. The group will have time for lunch and to buy food for the next days while the cars are being picked up (ca. 1h) and will travel to Kraków altogether by car. At AGH Kraków, students of the SGA Baltic student chapter will give a presentation about the geology of Poland.

- 12:33 arrival group in Katowice (main station)
- 12:35 arrival Cyrielle in Katowice (airport)
- 14:00 latest departure of the entire group (with both cars) from Katowice main station
- 17:00 hostel check-in (hopefully earlier)
- 18:00 meeting with students of the SGA Baltic student chapter at AGH Kraków



Wydział Geologii, Geofizyki i Ochrony Środowiska
aleja Adama Mickiewicza 30
GPS: 50°03'51.9"N 19°55'25.4"E
geol.agh.edu.pl



Old Walls Hostel
Grabowskiego 9A/7, Old Town
GPS: 50°04'00.6"N 19°55'37.5"E
<http://www.oldwallshostel.pl/indexen.html>

17.06.2018 - Wieliczka salt and Szklary gemstone mines

- 08:00 departure from hostel
- 08:30 visit to Wieliczka salt mine - tourist route (ca. 3 h)



Daniłowicz Shaft, Wieliczka salt mine
ul. Daniłowicza 10, Wieliczka
GPS: 49°58'58.0"N 20°03'22.0"E
<https://www.wieliczka-saltmine.com/>

- 11:30 lunch
- 12:00 drive to Szklary (ca. 3.5 h)
- 16:15 visit to Szklary gem stone mine (ca. 1 h)



Szklary gem stone mine
Sklary Huta, 5 km from Ząbkowice Śląskie
GPS: 50°38'45.1"N 16°49'39.5"E
<http://www.kopalniaszklary.pl/english.html#>



Wigwam Hostel
ul. Szybka 6-10, Krzyki
GPS: 51°06'09.5"N 17°03'14.9"E
<http://wigwam-hostel.wroclaw-hotels.com/>

18.06.2018 - Chromitites, University of Wrocław

On 18 and 19 June, two students from Wrocław University will join our group. They will be picked up and dropped off at Wrocław University. At the meeting with the Polish students in the evening, our group will give a presentation about our student chapter.

- 07:30 departure from hostel
- 08:00 meeting with Dr. Piotr Wojtulek and Polish students at University of Wrocław
- 17:00 meeting with Polish students at University of Wrocław
- 18:00 social evening with the Polish students



Institute of Geological Sciences
University of Wrocław
pl. Maksa Borna 9, Wrocław
GPS: 51°07'00.6"N 17°01'44.8"E
<http://www.ing.uni.wroc.pl/home-page>



Wigwam Hostel (as the day before)

19.06.2018 - KGHM Lubin Kupferschiefer mine

KGHM recently laid off one of their CEOs, resulting in some confusion within the company. We are lucky to get access, so being on time is essential! At the mine, we will change into miners' clothes (including lamps and breathing apparatus in case of fire) and receive a brief safety training. It will be dark, hot, and humid underground.

- 04:00 departure from hostel
- 04:30 meeting with Dr. Wojciech Śliwiński and Polish students at University of Wrocław (same place as before)
- 06:00 safety training at Lubin Główny
- 07:30 visit to Lubin Główny underground mine, mining section No. G5
- 12:00 lunch at the KGHM canteen



Lubin mine (Zakłady Górnicze Lubin)
ul. M. Skłodowskiej-Curie 188, Lubin
GPS: 51°24'59.0"N 16°11'13.8"E
<http://kghm.com/en/our-business/mining-and-enrichment/lubin>



Wigwam Hostel (as the day before)

20.06.2018 - Leisure day

Wrocław is a historically important and culturally versatile city. From the hostel, it is a ca. 25 min walk to the historic city center. See here for sight-seeing: <https://visitwroclaw.eu/en>. The group will meet at the hostel at 4 pm to drive to Bełchatów.

- 11:00 latest check-out of hostel
- 16:00 drive to Bełchatów (ca. 2.5 h)



Hotel i Restauracja Jan
77 Lipowa, Bełchatów
GPS: 51°21'33.2"N 19°21'06.5"E
<http://www.restauracja-jan.pl/>

21.06.2018 - PGE Bełchatów lignite mine

We will first go to the Directorate building to register and park the cars. Be prepared for an administrative nightmare. At PGE's Bełchatów and Szczerców lignite open pit mines, we will be guided by geologist Leopold Czarnecki (Leopold.Czarnecki@gkpgge.pl). The mine does not provide any clothes or security equipment. Taking pictures is strictly forbidden (except for viewing points indicated in the link below)!

- 08:00 departure from hotel
- 08:30 visit to Bełchatów (and possibly Szczerców) pits, ca. 3h
- 12:00 lunch at Bełchatów canteen
- 13:00 drive to hostel in Sosnowiec (ca. 3h)



PGE Mining and Conventional Power
(PGE Górnictwo i Energetyka Konwencjonalna S.A., Oddział KWB Bełchatów)
Św. Barbary 3, Rogowiec
GPS: 51°15'31.1"N 19°18'57.1"E
<https://kwbbelchatow.pgegiel.pl/Kontakt>



Hostel Mikołajczyka59
ul. Mikołajczyka 59, Sosnowiec
GPS: 50°15'19.3"N 19°08'57.8"E
<http://www.mikolajczyka59.pl/>

22.06.2018 - ZGH Bolesław's Pomorzany-Olkusz Pb-Zn mine

We will meet our guide (Tomek Cwiertnia, Wlodek Zygo, or Krzysiek Foltyn) from AGH Kraków at the gate of Pomorzany mine. You may get some nice samples here, so bring sampling bags.

- 07:15 departure from hostel
- 08:00 visit to Pomorzany underground mine



Kopalnia Pomorzany
GPS: 50°17'56.2"N 19°30'10.4"E
<http://www.zghboleslaw.pl/en/>



Hostel Mikołajczyka59 (as the day before)

23.06.2018 - Hard coal mine

The visit to PGG's Piast-Ziemowit hardcoal underground mine has been cancelled due to a mining accident (05.05.2018) related to an earthquake at JSW's Zofiówka mine. To extensively assess the mine stability and safety, PGG will not allow access to visitors until the end of 2018. We are currently looking for an alternative.



Option 1: PG Silesia's Silesia hard coal mine
<http://www.pgsilesia.pl/en/about-us/general-information>
<https://kopalniaguido.pl/index.php/en/>



Option 2: Guido coal mine
3 Maja 93, Zabrze
GPS: 50°17'21.3"N 18°47'34.6"E
<https://kopalniaguido.pl/index.php/en/>



Hostel Mikołajczyka59 (same as before)

24.06.2018 - Tarnowskie Góry mine

Leslie, Jeremias, and Cyrielle will return to Zurich/Toulouse. Leslie and Jemerias drop off one car at the airport in Kraków at night; Micha drops off the second car in the afternoon at Katowice main station.

08:30 departure from hostel
09:40 visit to Tarnowskie Góry mining museum
(90 min visit; arrival 15 min in advance)
12:00 drop off Cyrielle at Katowice airport
13:30 departure Cyrielle from Katowice airport
17:00 latest drop-off of car at Katowice main station



Historic Silver Mine at Tarnowskie Góry
(Zabytkowa Kopalnia Srebra)
ul. Szczęść Boże 81
GPS: 50°25'31.9"N 18°50'56.2"E
<http://kopalniasrebra.pl/en/touring/>



Hostel Katowice Centrum
ul. Andrzeja 19
GPS: 50°15'23.5"N 19°00'54.1"E
<http://www.hostelkc.pl/>

At the Tarnowskie Góry historic silver mine, we will have an English-speaking guide. The tour includes a visit to the mining museum, at 1740 m long underground walk, and a short boat ride.

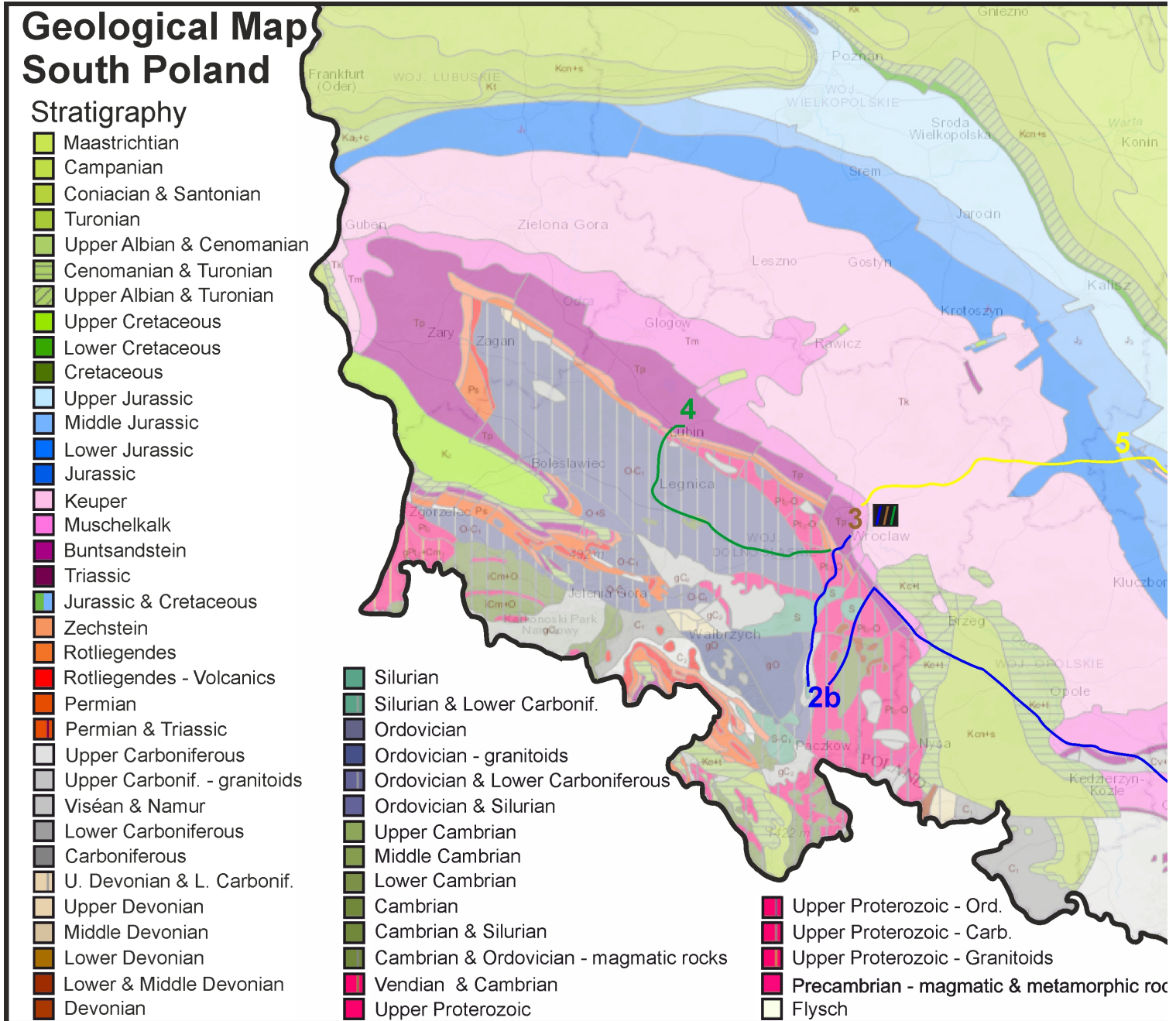
25.06.2018 - Return to Zurich

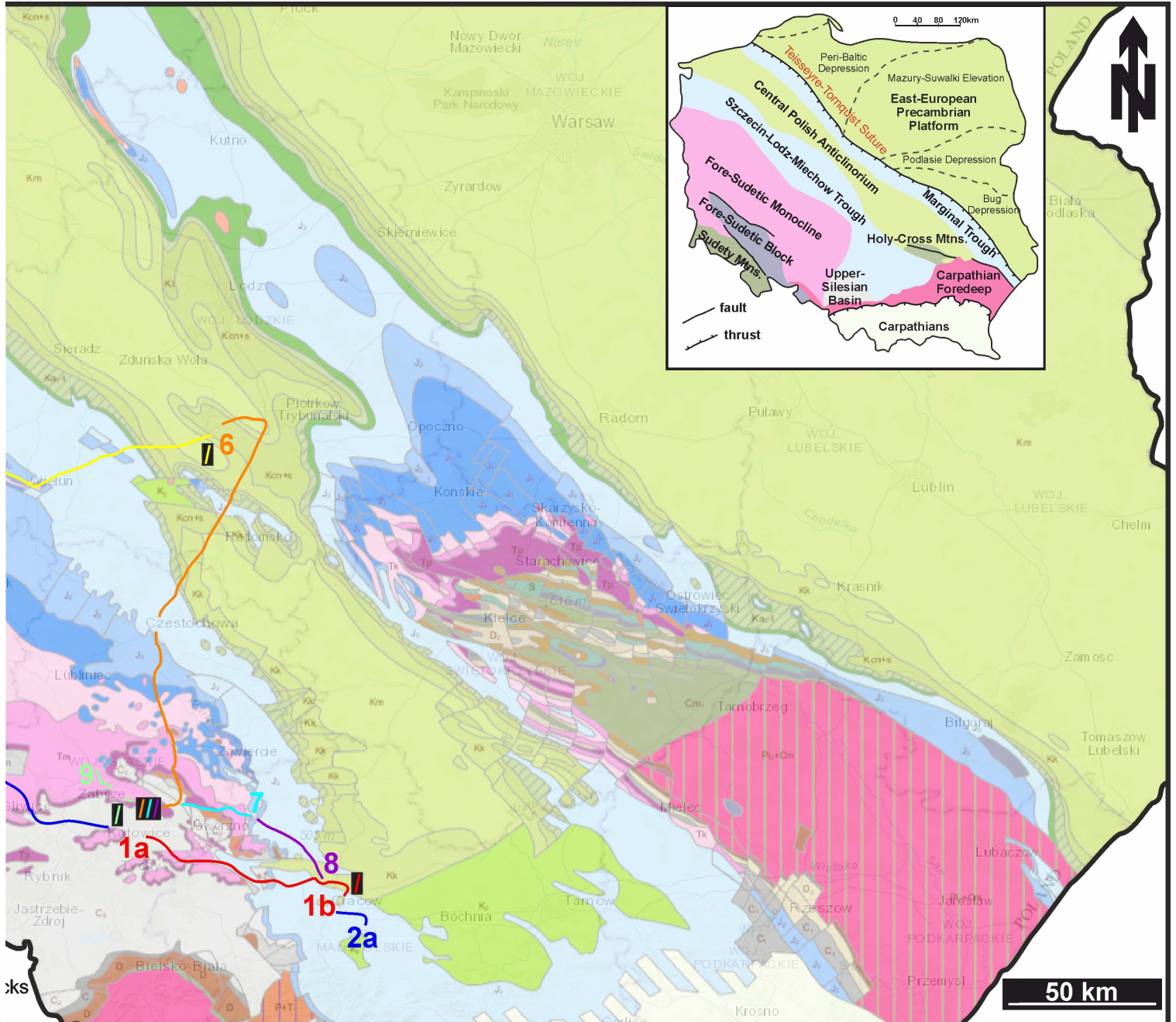
The hostel is located right next to Katowice main station. In Vienna, everybody is free to explore the city by themselves. The group meets again at the platform of Vienna main station at 9 pm.

Connection:

25.06. Katowice to Vienna, EC103 (seats)
09:25 - 13:49
Vienna to Zurich, NJ466 (couchette)
21:27 - 08:20 (+1 day)

Itinerary





Modified from Polish Geological Institute (<https://geolog.pgi.gov.pl/#>) and Redstone Exploration Services (<http://redstone-exploration.com/country-profiles/poland/>).

Geology of Poland

Alina Fiedrich

- Basement: East-European Craton (Baltica), Pomeranian Caledonides (Avalonia), Sudetes (Armorican Terranes), Carpathians (4 terranes, Alpidic)
- Polish Trough: Deposition of thick sedimentary successions, including Kupferschiefer and evaporites
 - Quaternary influenced by several glaciations

Basement

Four main geological units of Poland can be distinguished (Figure 1): (i) The Precambrian East-European (Fennosarmatian) Craton in the north-east, (ii) the Caledonian segment, (iii) the Variscan Sudetic block in the south-west (together forming the Paleozoic Platform), and (iv) the Carpathians in the south.

According to Bogdanova et al. (2005), the East European Craton (EEC; pink in Figure 1) is composed of Precambrian continental crust of ca. 30-40 km thickness. It comprises three segments, Fennoscandia in the west (roughly Poland, Sweden, Finland), Sarmatia in the south (roughly Ukraine), and Volgo-Uralia in the north-east (roughly Russia), which were amalgamated in the Paleo-Proterozoic and are now separated by Meso-Neoproterozoic rifts. The western segment of the EEC is a remnant of the paleo-continent Baltica

and is limited to the west by the northwest-southeast striking Teisseyre-Tornquist Suture (TTS; part of the Transeuropean Suture Zone). It exhibits orogenic belts with voluminous post-collisional granites (Bogdanova et al., 2005).

The Paleozoic Platform comprises a Caledonian and a Variscan section (blue and green in Figure 1, respectively). According to Mazur et al. (2016), the paleo-continent Avalonia attached to Baltica during the Ordovician, giving rise to the Caledonian orogeny. The plate boundary is likely located toward the west or south-west of the Precambrian TTS. This zone is also referred to as the Pomeranian Caledonides (Mazur et al., 2016).

According to Mazur et al. (2006) and references therein, the Variscides of Poland developed due to amalgamation of the Armorican terranes to Baltica and

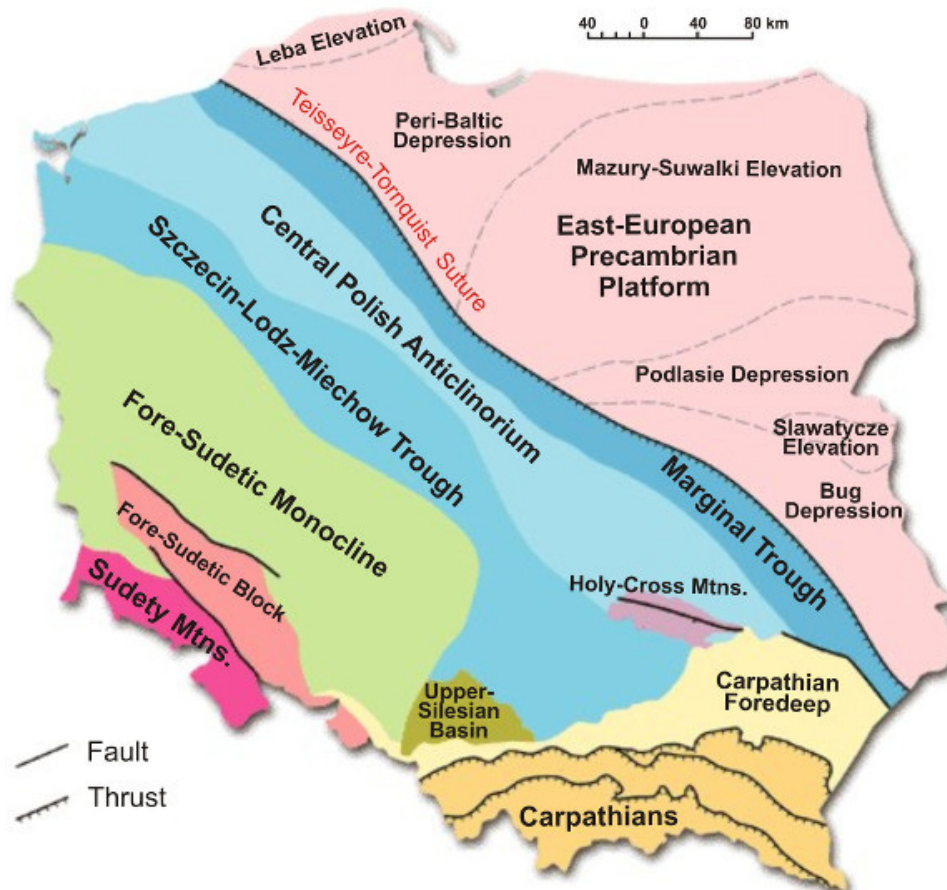


Figure 1: Simplified, schematic map of the four main geological units of Poland, from Redstone E.S. (2018).

Avalonia during the Devonian to Early Carboniferous (Figure 2). They comprise the metamorphic internides and the fold-and-thrust belt of the externides. The externides are represented by the Sudetes, which in turn are separated into the Sudete Mountains and the Fore-Sudetic Block (pink in Figure 1). The Sudetes comprise a mosaic of terranes of Neoproterozoic to Devonian protoliths dominantly built of volcano-sedimentary successions with variable metamorphic overprint, igneous suites, and late- to post-orogenic granites (Mazur et al., 2006, and references therein). The highest peak of the Sudetes is Śnieżka (1603 m) in the Karkonosze Mountains at the border between Poland and Czech Republic. The fold-and-thrust belt mostly comprises Carboniferous syn- to post-orogenic turbidites. It is buried under the thick Permo-Mesozoic sedimentary cover of the Polish Trough (Mazur et al., 2006).

The Upper Silesian Basin (brown in Figure 1) can essentially be regarded as a foreland basin of the Variscides, although key structures may have already been initiated during the Cadomian stage and its structural

development was also influenced by the Alpine stage (Dopita and Kumpera, 1993). The basin is filled with sandstones, carbonates, and various molasse sediments. Notably, extensive coal beds (Carboniferous) occur under the Outer Carpathian nappes (Dopita and Kumpera, 1993).

The Carpathians (yellow in Figure 1) are an Alpine orogen that formed during Mesozoic-Tertiary times. They are separated into the internides, consisting of four terranes (Alcapa, Tisza, Dacia, and Adria, each assembled during Jurassic to Paleogene times) and the external Alpine-Carpathian Flysch belt (Csontos and Vörös, 2004). Southeast Poland is composed of the latter and only little of the internides reaches Polish territory. The Flysch belt is a Tertiary accretionary prism, with an inner Alcapan section and an outer European section (Csontos and Vörös, 2004, and references therein). Both the Flysch belt and the foreland deep, formed by Flysch nappes thrust over the Carpathian foreland, are economically significant for their petroleum reserves (Poprawa et al., 2015).

The Polish Trough

The Polish Trough (also referred to as Polish Basin) forms the eastern part of the Central European Basin (Figure 3) and adjoins the EEC in the east. According to Walter (2007) and references therein, northwest-southeast oriented graben structures, which developed during the Permian, essentially formed the trough. Subsidence intensified in the early Mesozoic and ceased toward the Upper Cretaceous due to Alpine compression. The up to 10 km thick, dominantly Permian-Mesozoic sedimentary deposits of the Polish trough cover parts of both the EEC and the Caledonides. During Devonian-Permian times dominantly marine deposits formed. Economically significant

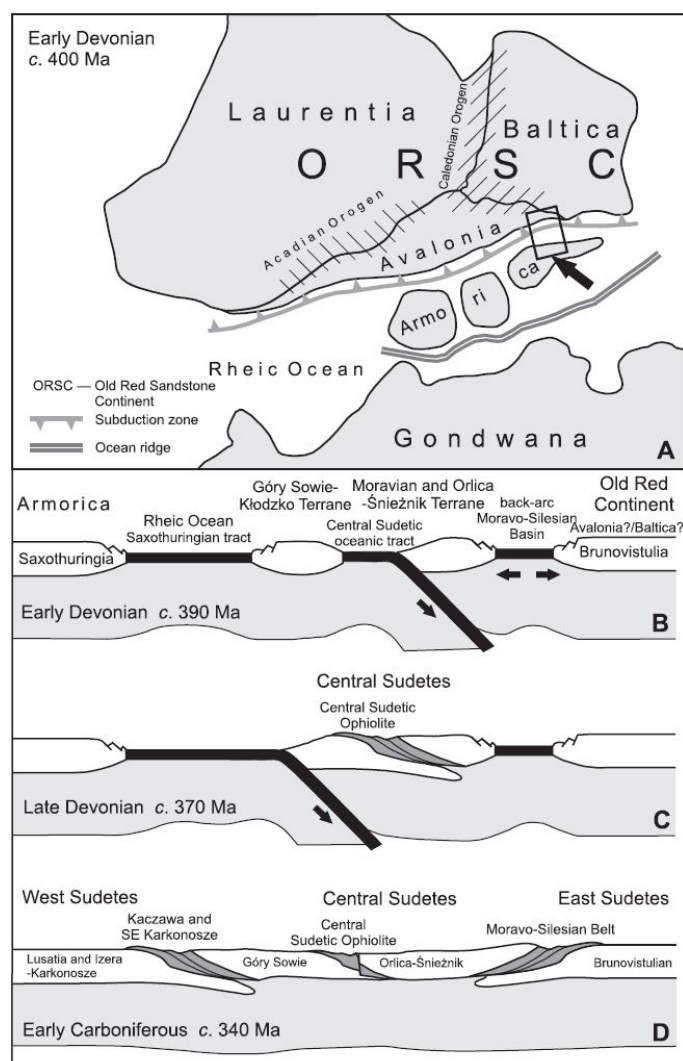


Figure 2: Simplified geodynamic scenario of the formation of the Sudetes, from Mazur et al. (2006).

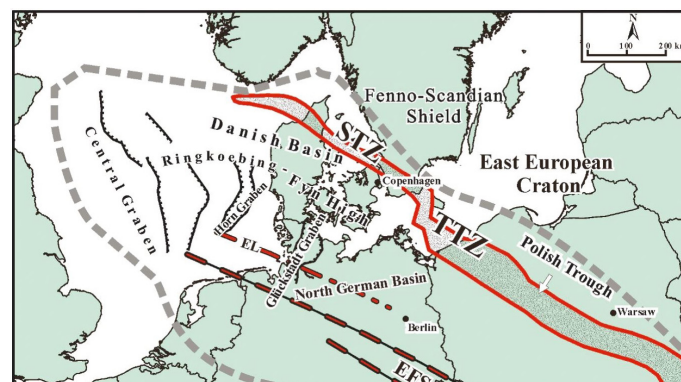


Figure 3: Overview over the Central European Basin from Cacace et al. (2008). STZ = Sorgenfrei-Tornquist-Zone; TTZ = Teisseyrie-Tornquist-Zone; EFS = Elbe Fault System; RFH = Ringkøbing-Fyn-High; EL = Elbe Lineament.

units include Carboniferous coal-bearing sandstones and mudstones, the Kupferschiefer marine clay, and Zechstein evaporitic salts. During Mesozoic times deposition of continental sandstone, shallow-marine sediments, and Upper Cretaceous chalcstone dominated (Walter, 2007, and references therein).

Quaternary

As many as eight Pleistocene glaciations can be traced in Poland, but only the last two (Odranian and Vistulian) are visible in the modern landscape (Figure 4; Marks, 2011).

According to Marks (2002) and references therein, the maximum extent of the ice sheets (Figure 4) can be determined from geomorphological features in the landscape. These include glacial tunnel lakes, end moraines, and outwash plains. In addition, the extent of glacial tills and its composition are used to distinguish different glacial phases. From the orientation of streamlined landforms such as drumlins, glacial tunnel valleys, and eskers, ice-flow directions can be determined.

The last glacial maximum (LGM) in Poland occurred at 24-16 ka BP (Marks, 2012, and references therein). It is also termed Vistulian or Wisła (German Weichsel) glaciation and is separated into three phases: Leszno, Poznań, and Pomeranian. Several ice lobes advanced from the Baltic Basin and, although they did not extend further than to central Poland, their effects



Figure 4: Extent of Pleistocene glaciations in Poland, from Marks (2004); O = Odranian, W = Wartanian, mV = middle Vistulian, L = Leszno phase, Pz = Poznan phase, Pm = Pomeranian phase.

are visible further south: Melt water runoff generated sandur trains, ice-marginal spillways, and proglacial lakes (Marks, 2002).

References

- Bogdanova, S.V., Gorbatshev, R., and Garetsky, R.G. (2005): East European Craton. In: Selley, R.C., Cocks, L.R.M., and Plimer, I.R. (eds): *Encyclopedia of Geology*.
- Cacace, M., Bayer, U., Marotta, A.M., and Lempp (2008): Driving mechanisms for basin formation and evolution. In: Littke, R., Bayer, U., Gajewski, D. and Nelskamp, S. (eds): *Dynamics of Complex Intracontinental Basins*. Springer, Berlin, Heidelberg.
- Csantos, L. and Vörös, A. (2004): Mesozoic plate tectonic reconstruction of the Carpathian region. *Palaogeography, Palaeoclimatology, Palaeoecology* 210, 1-56.
- Dopita, M. and Kumpera, O. (1993): Geology of the Ostrava-Karviná coalfield, Upper Silesian Basin, Czech Republic, and its influence on mining. *International Journal of Coal Geology* 23, 291-321.
- Marks, L. (2004): Pleistocene glacial limits in Poland. In: Ehlers, J. and Gibbard, P. L. (eds): *Quaternary Glaciations - Extent and Chronology*. Elsevier, Amsterdam.
- Marks, L. (2002): Last Glacial Maximum in Poland. *Quaternary Science Reviews* 21, 103-110.
- Marks, L. (2004): Pleistocene glacial limits in Poland. *Developments in Quaternary Sciences* 2, 295-300.
- Marks, L. (2011): Quaternary Glaciations in Poland. *Developments in Quaternary Sciences* 15, 299-303.
- Marks, L. (2012): Timing of the Late Vistulian (Weichselian) glacial phases in Poland. *Quaternary Science Reviews* 44, 81-88.
- Mazur, S., Aleksandrowski, P., Kryzna, R., and Oberc-Dziedzic, T. (2006): The Variscan Orogen in Poland. *Geological Quarterly* 50, 89-118.
- Mazur, S., Mikolajczak, M., Krzywiec, P., Malinowski, M., Lewandowski, M., and Buffenmyer, V. (2016): Pomeranian Caledonides, NW Poland - A collisional suture or thin-skinned fold-and-thrust belt? *Tectonophysics* 692, 29-43.
- Poprawa, P., Hendel, J., Sikora, A., and Kuczyński, S. (2015): Geological setting and gas/oil exploration potential of Poland. 15th International Multidisciplinary Scientific GeoConference SGEM 1, 189-205.
- Redstone Exploration Services (2018), accessed 10.06.2018: Poland. <http://redstone-exploration.com/country-profiles/poland/>.
- Walter, R. (2007): *Geologie von Mitteleuropa*. Stuttgart, Schweizerbart, 7th ed.

The Wieliczka salt mine

Jakub Sliwinski

- The Wieliczka salt mine was an important part of Polish mining from the 13th century till its closing in 2007.
- Rock salt deposits were formed in evaporitic basins during the Badenian salinity crisis in the Miocene (~12 Ma) in the foreland of the Carpathian thrust.
- Evaporites (anhydrite-halite) formed cyclically in 5 stages to a thickness of 40-200 m and are hosted between two clastic sedimentary layers comprising claystones and siltstones.
- Deformation during the Carpathian (Alpine) orogeny uplifted the deposits, making the evaporite beds accessible for mining.

Salt mining history

The evaporitic rock salt deposits of the Carpathian foreland in southern Poland, which notably host the Wieliczka and Bochnia mines south of Kraków, have been an important part of Polish mining for centuries, if not millennia. Evidence of salt production in the area is perhaps as old as ~3,500 BC, beginning as the evaporation/boiling of saline springs and progressing to the discovery and mining of rock salt in the mid-13th century (Garlicki, 2008). Given the high value of salt in medieval times, the mines of Wieliczka and Bochnia were held under royal domain and produced approximately one third of the treasury's revenue in the 14th and 15th centuries (Hallett, 2002).

While the mine at Wieliczka is no longer operating as of 2007, its long tenure as an active mine and its importance to the region earned it a spot on the first list of UNESCO World Heritage sites in 1978. Nowadays it is still operational as a tourist attraction, showcasing both the geology of the salt deposit as well as artistic works carved out of the caverns (Figure 1).

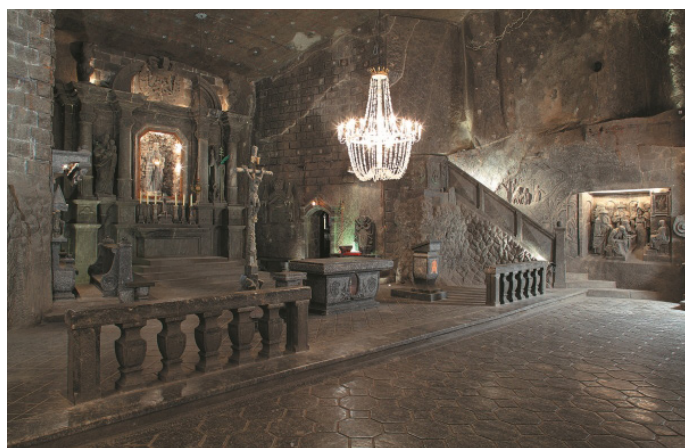


Figure 1: Chapel of St. Kinga at Wieliczka salt mine. From Wieliczka Salt Mine (n.d.).

Salt deposition

The two deposits are Miocene in age (upper Badenian, 11.1-13.4 Ma; Bąbel, 2004, and references therein) and are comprised of several cycles of deposition following a salinity crisis. In particular, global cooling, combined with dropping sea levels following the Miocene climatic optimum (Bąbel, 2004) led to the total or partial isolation of sedimentary basins in the Carpathian foreland (Figure 2). Located atop flysch sediments from the alpine overthrust, these basins became repeatedly saturated in brine-related elements (e.g., Ca^{2+} , Na^+ , SO_4^{2-} , Cl^-) and diluted by meteoric input over time, leading to the deposition of extensive



Figure 2: Distribution of Miocene (Badenian) evaporites in the Carpathian foreland (Bąbel, 2004; modified after Khrushov and Petrichenko, 1979 and Garlicki, 1979). Wieliczka and Bochnia mines located in inset.

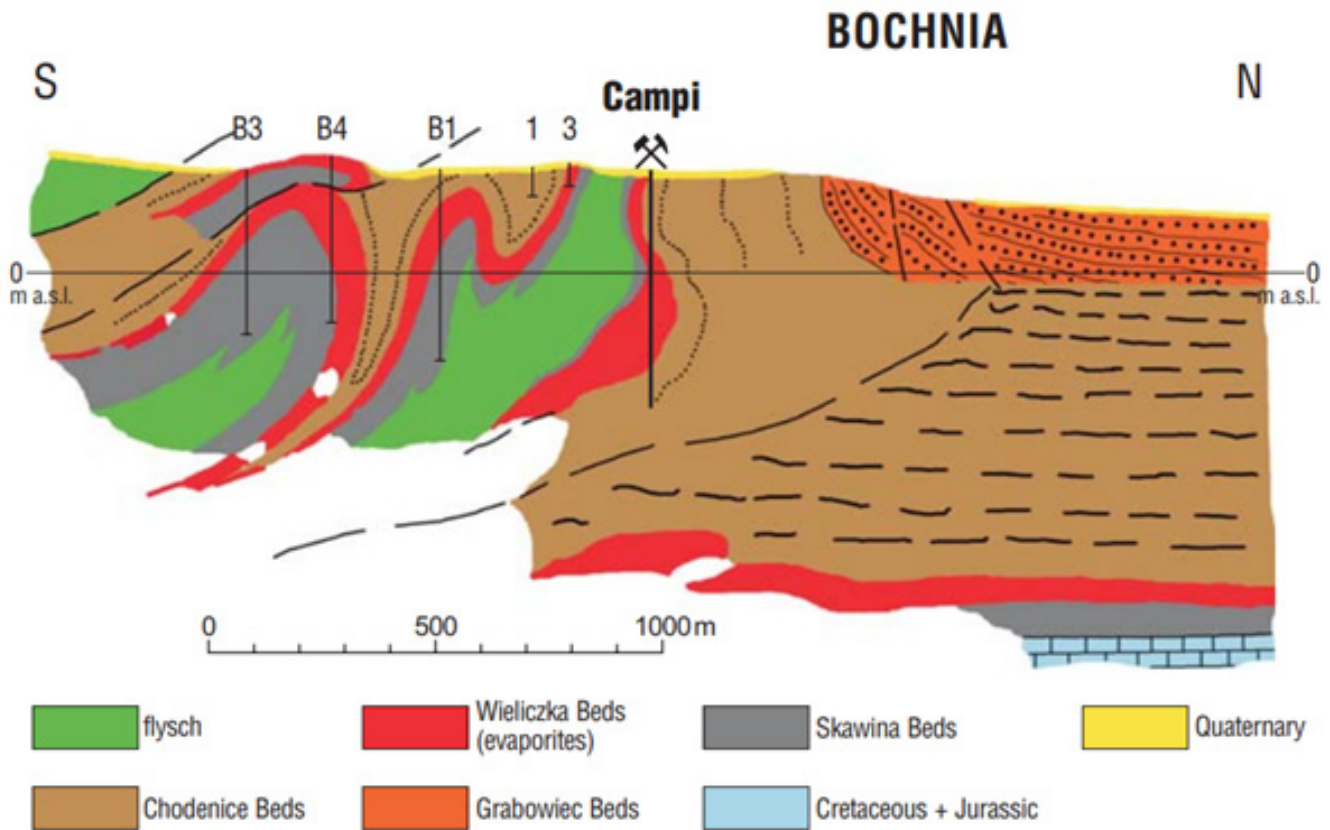


Figure 3: Schematic cross section of the Campi mine shaft at Bochnia (Garlicki, 2008).

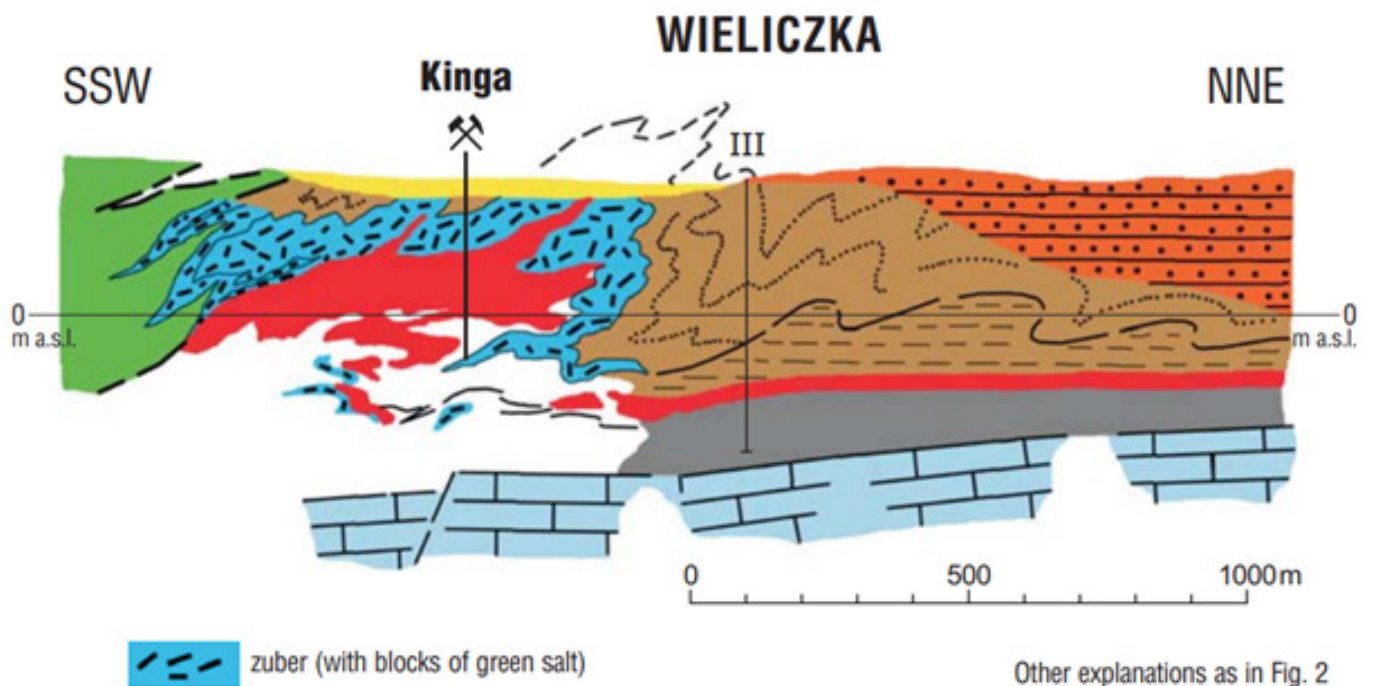


Figure 4: Schematic cross section of the Kinga mine shaft at Wieliczka (Garlicki, 2008).

evaporitic deposits in modern-day Poland, Ukraine and Romania. These deposits vary in thickness from 100's of meters in the west to over 3,000 m in the east (Figure 2), and are divided into three subunits, with the evaporites intercalated between two clastic sedimentary beds: the clastic Skawina beds underlie the salt-bearing Wieliczka beds, which in turn underlie the clastic Chodenice beds (Figures 3 and 4).

Stratigraphy

The Skawina beds are comprised of marly claystones, marly-clayey shales and rarely, siltstones with evaporitic cements. These beds range in thickness between 1-150 m and transition into the overlying Wieliczka evaporites, which in turn transition into the top-most Chodenice beds of similar composition to the Skawi-

na (100-1,000 m of sandy, marly, and clayey shales). The Wieliczka evaporites sandwiched between these two formations can be subdivided into 5 cyclothem that together measure 40-200 m in thickness (increasing eastward). Each cyclothem begins with claystone-anhydrite rocks mixed with silt and carbonized plant fragments, which gradually become banded and then laminated toward the top of the succession (Garlicki, 2008). The upper part of the first four cyclothem is comprised of chloride (rock salt) facies, while the last contains a layer of anhydrite. Following deposition, the Wieliczka beds, together with their under- and over-lying units, were extensively deformed during the Carpathian (Alpine) overthrust, forming anticlinal structures that were partially exhumed and thereby accessible to miners. The salt that was mined in these areas is hosted in highly-folded and deformed layers of the allochthonous strata, while the autochthonous strata remain at depth.

The salt deposit at Wieliczka measures about 1 by 6 km in horizontal extent and lies approximately 400 m underground. This deposit is subdivided into two parts, including an upper “boulder deposit” (salty clays with blocks of coarse “green” salt), and a lower “stratified” or “bedded” layer consisting of strongly folded salt layers (Figure 5). While the upper deposit is thought to occur as a result of gravitational slumping during deformation of the sedimentary beds, the lower deposit contains a complex and resolvable sequence of layers, including anhydritic claystones and siltstones variably intercalated with salts (Figure 5; Garlicki and Wiewiórka, 1981).

References

Bąbel, M. (2004): Badenian evaporite basin of the northern Carpathian Foredeep as a drawdown salina basin. *Acta Geologica Polonica* 54, 313-337.

Durska, E. (2018): The Badenian Salinity Crisis in the palynological record: vegetation during the evaporative event (Carpathian Foredeep, southern Poland). In: *Annales Societatis Geologorum Poloniae*, vol 87. pp 213-228.

Garlicki, A. (2008): Salt mines at Bochnia and Wieliczka. *Przegląd Geologiczny* 56, 663-669.

Garlicki, A. and Wiewiórka, J. (1981): The distribution of bromine in some halite rock salts of the Wieliczka salt deposit (Poland). In: *Annales Societatis Geologorum Poloniae*, vol 51. pp 353-359.

Hallett, D. (2002): The Wieliczka salt mine. *Geology Today* 18, 182-185.

Wieliczka Salt Mine (n.d.), accessed 05.06.2018:

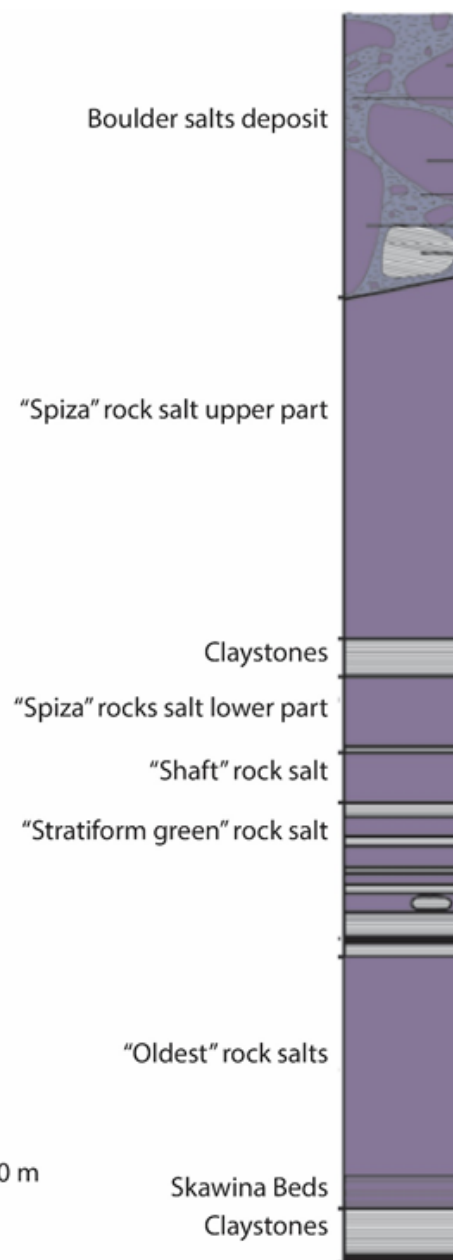


Figure 5: Schematic stratigraphic profile of the Wieliczka salt deposits, with miners' terminology in quotes. Modified after Durska (2018) and Garlicki and Wiewiórka (1981).

The Szklary gemstone mine

Julian Reyes

- The largest nickel reserve in Poland
- Silicate-type nickel deposit (nickel-bearing serpentinite), formed by hydrothermal and later lateritic weathering of ultramafic rocks (peridotites).
- First known occurrence of chrysoprase (green Ni-chalcedony)

Introduction

The mine is located 142 km south-west of Warsaw in Szklary, Kłodzko County, Poland. The deposit has been mined for chrysoprase since the Middle Ages. Nickel exploration started in 1891 by underground tunnels. From 1935 open pit mining was the main method for extraction until the mines were abandoned in 1980. Currently the site serves as a museum, where the main attractiveness for tourists and gem collectors is the appearance of green quartz (chrysoprase) (Figure 3). Chrysoprase is found in thick veins which are hosted in altered ultramafic rocks. Sometimes these veins are overlain by a saprolite cover enriched in clay minerals, particularly smectite. Furthermore, some pegmatitic and oligoclastic veins associated with the Variscan syenite massif cross cut the deposit (mindat.org, 2018).

Geological setting

The deposit is hosted in ultrabasic rocks (Figure 1) that are from the lowest member of Lower Paleozoic Ophiolite Suite, known also as the Sudetic Ophiolite (Dubińska and Gunia, 1997; Majerowicz and Pin, 1989, 1994). The ultramafics are composed of weakly serpentinitized ultrabasites, harzburgites, lherzolites and pyroxenites. However, in the sequences there are also reported plagiogranite intrusions, trondhjemites. The silicate layers from Szklary massif have a complex origin consisting of two events: (1) hydrothermal metamorphism related to the serpentinitization of ultramafic rocks and posterior metamorphism, where serpentine, chlorite and clintonite precipitated (Figure 2); (2) hydrothermal and supergene alteration of ultrabasic rocks and various metamorphic schists (Figure 2) (Dubińska et al., 2000). Pegmatites found on the Szklary massif are associated to the partial melting of old sedimentary rocks during high grade metamorphism (Pieczka, 2000).

Chrysoprases from Lower Silesia often occur as high-angle veins in brownish-red weathering material derived from serpentinites (Figure 3). Associated with

these veins there are other greenish minerals, due to the high content of Ni, such as nimitite and pimelite. Although most of the chrysoprase (95%) is chalcedony, there are important inclusions of chrome spinel and magnetite (Korybska-Sadło, 2015).

A study by Michalik (2000) shows that gold concentration on the Szklary massif has similar characteristics to laterite weathering. The weathering leads to secondary gold accumulation in the oxide zone and the water-table level. There is a correlation between gold and talc rocks, such as with chalcedony veins. However, gold is in low concentrations, and currently uneconomical.

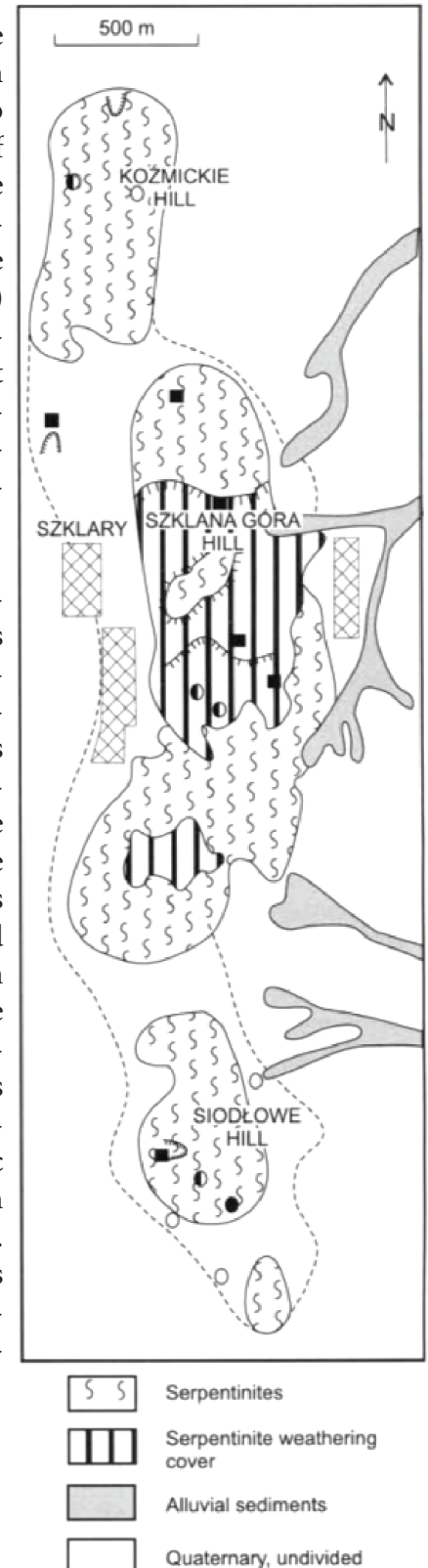


Figure 1: Geological map of the Szklary massif (simplified) from Gunia (2000).

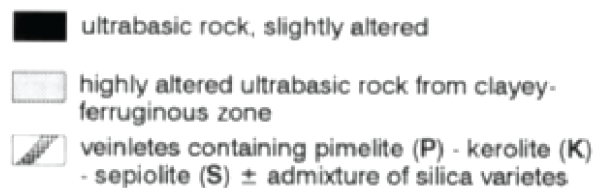
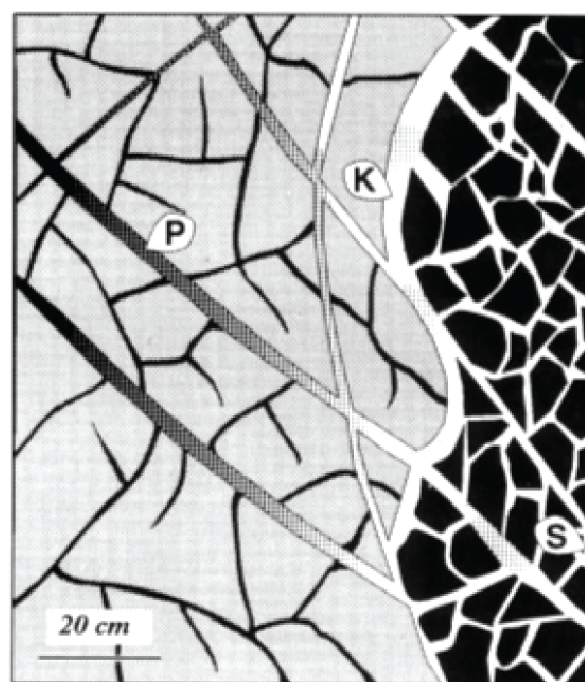
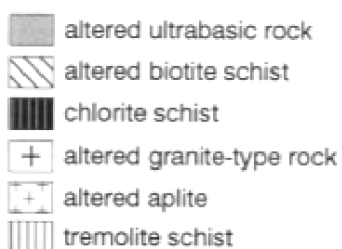
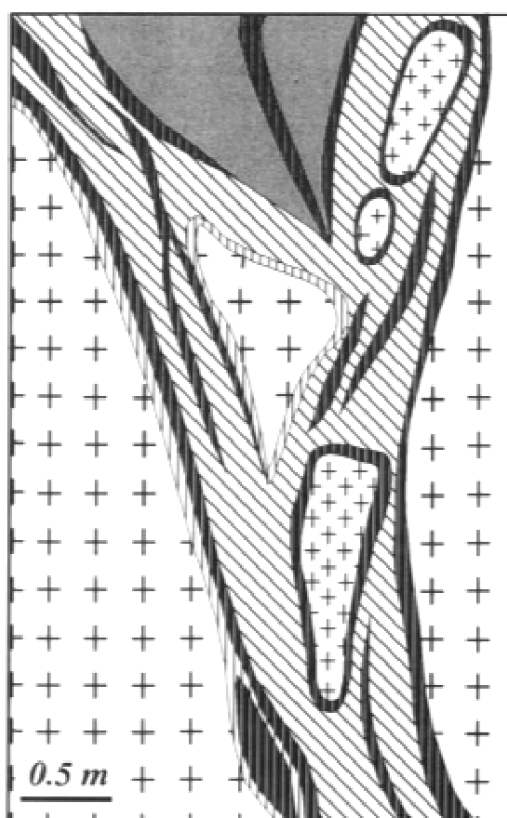
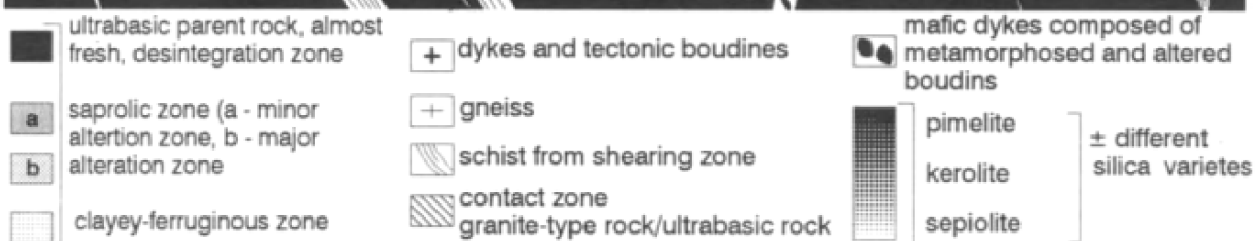
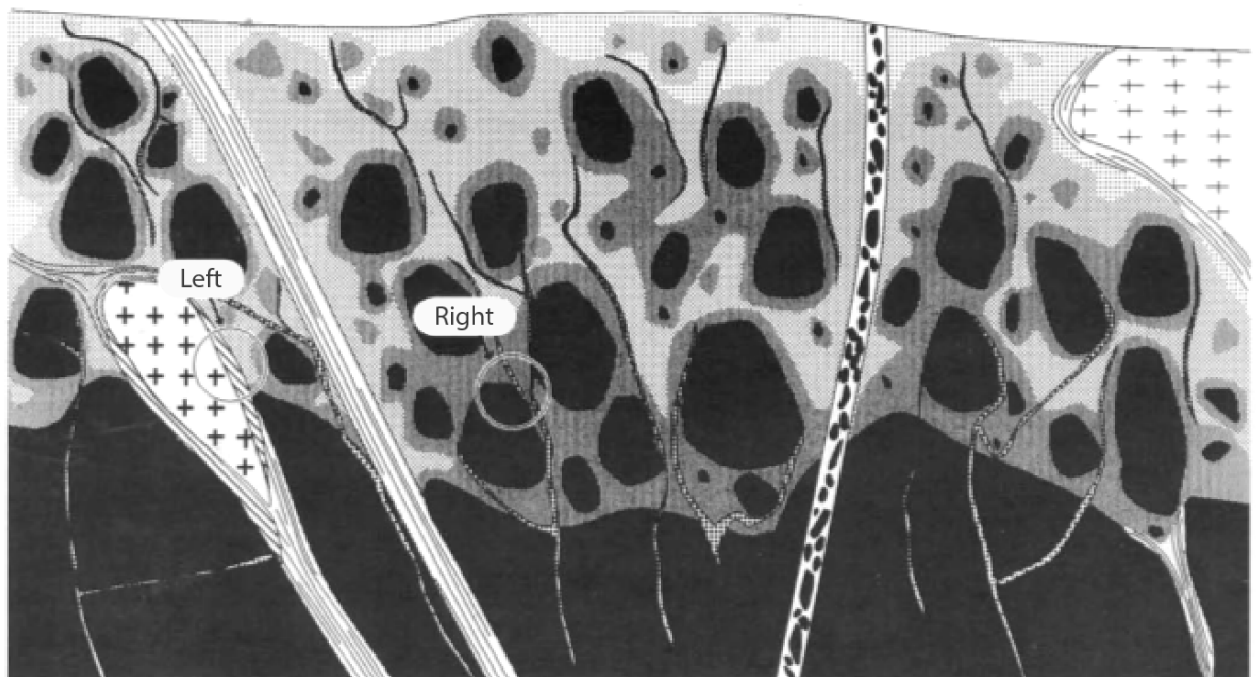


Figure 2: (top) Schematic geological cross-section of the weathering crust from Szklary. (bottom) Sketch of the occurrence of: (left) contact zones between ultrabasic and granite-type rocks and (right) sepiolite-kerolite-pimelite veins in variously altered ultrabasic rocks. Taken from Dubińska et. al. (2000).

References

Dubińska, E. and Gunia, P. (1997): The Sudetic ophiolite: current view on its geodynamic model. *Geological Quarterly* 41, 1–20.

Dubińska, E., Sakharov B. A., Kaproń, G., Bylina, P., and Kozubowski, J. A. (2000): Layer silicates from Szklary (Lower Silesia): from ocean floor metamorphism to continental chemical weathering. *Geologia Sudetica* 33, 85–105.

Gunia, P. (2000): The petrology and geochemistry of mantle-derived basic and ultrabasic rocks from the Szklary massif in the Fore-Sudetic Block (SW Poland). *Geologia Sudetica* 33, 71–83.

Korybska-Sadło, I. (2015): Studies of chrysoprase and microcrystalline silica varieties from serpentinites of Szklary massif (Foresudetic block, sw Poland) by Raman spectroscopic technique – preliminary results. *Mining Science* 22, 39–45.

Majerowicz, A. and Pin, C. (1989): Recent progress in petrologic study of the Ślęza Mt. ophiolite complex, Lower and Upper Paleozoic Metabasites and Ophiolites of the Polish Sudetes, Multilateral Cooperation of Academies of Sciences of Socialist Countries, Problem Commission IX: Earth's Crust — Structure Evolution, Metallogeny, Project 2 and 7, 3. *Guidebook of Excursion in Poland*, 34–72.

Majerowicz, A. and Pin, C. (1994): The main petrological problems of the Mt. Ślęza ophiolite complex, Sudetes, Poland. *Zentralblatt für Geologie und Paläontologie* 1, 989–1018.

Michalik, R. (2000): Gold in the serpentinite weathering cover of the Szklary massif, Fore-Sudetic Block, SW Poland. *Geologia Sudetica* 33, 143–150.

Mindat.org (2018), accessed 10.06.2018: Szklary Chrysoprase Mine, Szklary (Gläserndorf), Ząbkowice (Frankenstein), Ząbkowice Śląskie District, Lower Silesia (Dolnośląskie), Poland. <https://www.mindat.org/loc-232015.html>.

Pieczka, A. (2000): A rare mineral-bearing pegmatite from the Szklary serpentinite massif, the Fore-Sudetic Block, SW Poland, *Geologia Sudetica* 33, 23–31.

Sachanbiński, M., Piórewicz, R., and Michalik, R. (2000): Heavy minerals in the serpentinite weathering cover of the Szklary massif, *Geologia Sudetica*, Vol. 33, pp. 131–141.

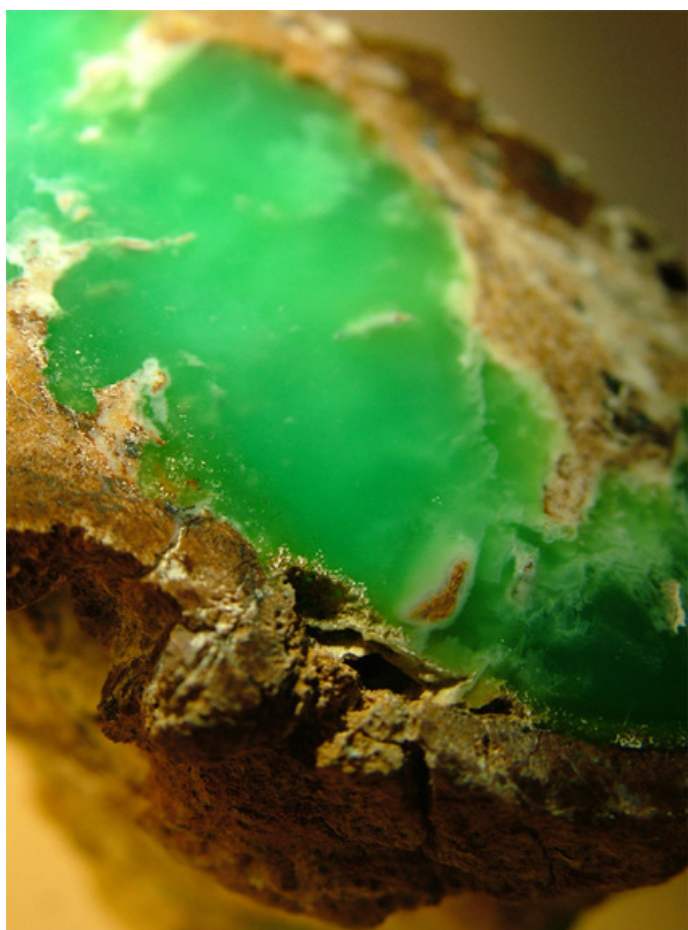


Figure 3: Mineral specimens found on Szklary mine. (top) Nimite. (middle) Chrysoprase. (bottom) Pimelite.

The Lower Silesian Chromitites

Maria Paula Castellanos Melendez

- Chromitites, with more than 90% chromite, and other Cr-ores occur in serpentinitised harzburgites in the Gogolów-Jordanów and Braszowice-Brzeznica massif, Lower Silesia (SW Poland).
- Chromitites crystallize from basaltic melts that migrate through dunite channels from different sources through the Moho Transition Zone.
- Cr-ore occurs as massive, laminated, nodular, disseminated, brecciated bodies or veinlets that have formed in an arc setting, in a supra-subduction zone.

Introduction

Chromitites are rocks containing more than 90% chromite, mainly Cr- and Al- rich spinel, and are associated worldwide with ophiolites, which are sections of the oceanic crust and upper mantle emplaced on land. Chromitites are commonly found in the upper mantle section or the crust-mantle boundary and are an important source of chromium. However, the chromite composition, its crystallization mechanism and their relationship with the tectonic setting is still a matter of debate (Wojtulek et al., 2016; González-Jiménez et al., 2014).

Geological setting

The Bohemian Massif is located in central Europe, near the eastern edge of the Variscan belt, and hosts chromitites in serpentinites within the Variscan ophiolitic sequence (Figures 1A and 1B). The most prominent assemblage of mafic-ultramafic bodies in the Bohemian Massif comprises three large massifs: Sleza, Nowa Ruda and Braszowice (Kryza & Pin, 2010).

The Sleza ophiolite is the largest preserved ophiolite and consists of serpentinites and serpentinitised rocks rich in pyroxene and amphibole from the Gogolów-Jordanów Serpentinite Massif (GJSM), metagabbros, amphibolites and metamorphosed dark radiolarian chert (Figure 1C). These rocks have been interpreted as mantle peridotites, ultramafic cumulates, gabbros, volcanic members with sheeted dyke complex, pillow lavas and oceanic sediments. The GJSM consists mainly of serpentinitised peridotites with some small plagiogranitic and rodingitic bodies and ophicarbonates. These rocks have been affected by regional metamorphism under greenschist-lower amphibolite facies conditions (Wojtulek et al., 2016).

The Braszowice-Brzeznica Massif (BBM) is located in the south end of the Niemcza Dislocation Zone. It consists of mantle serpentinites and moderately de-

formed gabbros (serpentinites with abundant relicts of olivine and tremolite, lizardite-chrysotile serpentinite, and antigorite serpentinites, Kryza & Pin, 2010), serpentinitic-magnetitic-dolomitic breccias, magnetite accumulations, rodingite and pyroxenite veins (western area), and aplite veins near granitic intrusions (eastern area, Figure 1D).

Chromitites

Chromitite bodies occur in the GJSM within strongly serpentinitised mantle harzburgite or dunite, which preserve altered olivine with mesh texture, abundant bastites after former enstatite, and interstitial clinopyroxene, olivine and spinel. Chromitites are found as pockets and veins within serpentinites of Czernica Hill. Mined pockets are mostly massive chromitite, have a stock morphology, irregular boundaries and sizes of 8-12 x 3-4 x 2-4 m. Chromite-bearing veins are smaller bodies close to larger pockets and were found to be up to 22 m long and 2 m thick. The ore bodies are surrounded by alteration zones with less chromian spinel. Chromitites occur as: massive (up to 90% chromian spinel; Figure 2A); laminated (up to 50% chromian spinel with chromite and chlorite-serpentine lamella); nodular (30 to 90% chromian spinel consisting of rounded chromian grains in a chlorite groundmass; figure 2B); disseminated (up to 15% chromite as small rounded grains in serpentinitic groundmass; Figure 2C); brecciated (Figure 2B) or veinlets (irregular and amoeboid bodies in serpentinite). The bulk rock composition of the chromitites show a harzburgitic and lherzolitic composition. Major element bulk-rock composition of the chromitites varies depending on the chromian spinel content, and shows a negative correlation between SiO₂ and MgO with the chromite ore. Trace element patterns show a characteristic feature with very low PGE content (42-79 ppb total PGEs, Wojtulek et al., 2016).

Chromite grains are divided in two generations: chromite I occurs predominantly in the massive ores in

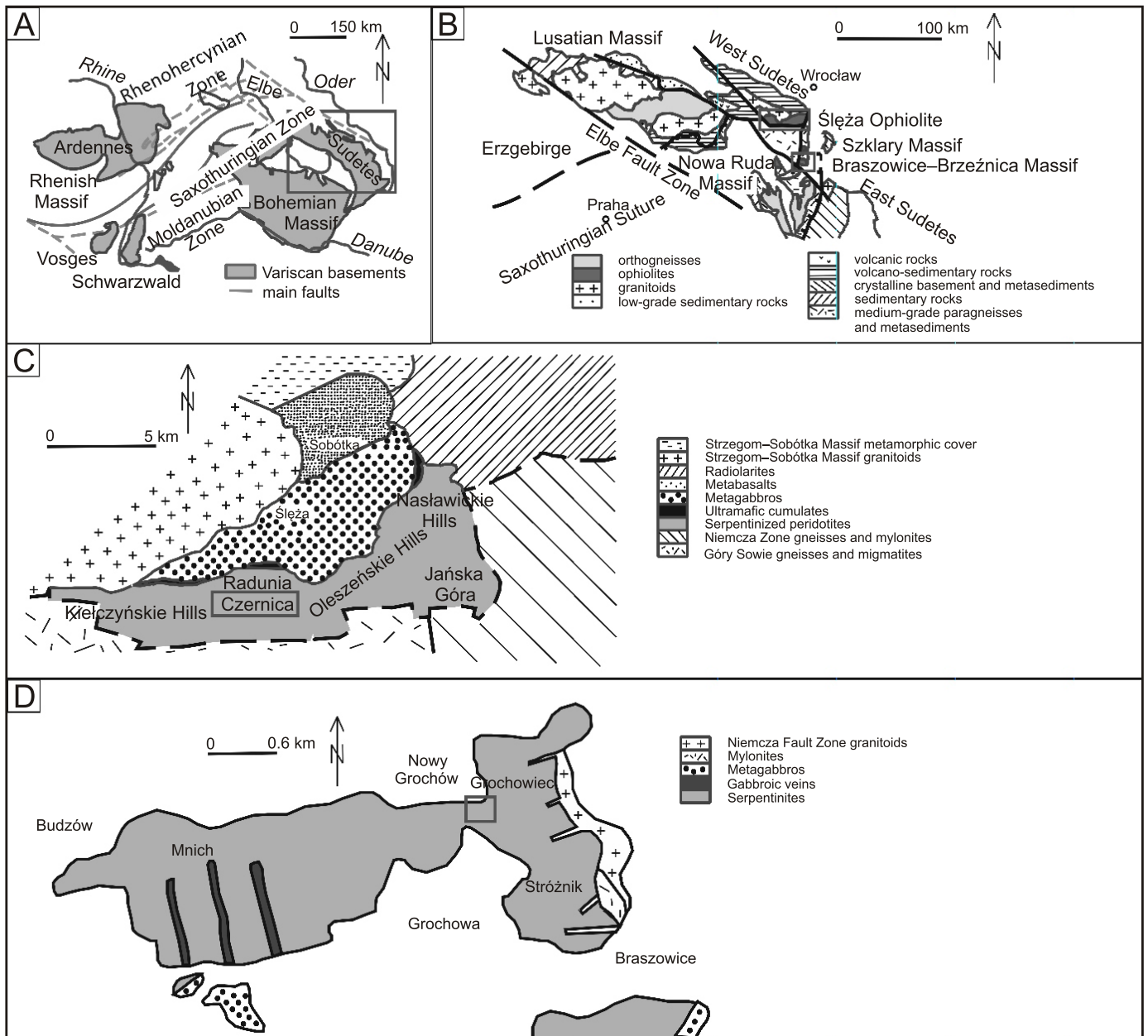


Figure 1: A - Location and geological setting of the Variscan orogeny in Central Europe; B - Geological setting of the Bohemian Massif (northern area); C - Geological units of the Sleza ophiolite, Gogolów-Jordanów Serpentinite Massif; D - Geological units of the Braszowice-Brzeznicza Massif (Wojtulek et al., 2016).

the core of the grains, and is surrounded by chromite II (Figure 2D). This first generation is richer in Al relative to chromite II and have Mg# 0.61-0.70, Cr# 0.50-0.52 and more consistent compositions in Cr# vs TiO₂. Chromite II is found in rims and fracture zones, commonly in nodular or disseminated ores. It has Mg# 0.57-0.69 and Cr# 0.39-0.63. Chlorite is almost purely magnesian with variable Al₂O₃. And the olivine in the serpentinite has forsterite content between 93 and 96 mol%. Millerite, godlevskite, polydymite and violarite, Ni and Fe-Ni sulphides, are also found in the chromitites (Wojtulek et al., 2016).

Cr-ore in the BBM is found as massive, brecciated, nodular or disseminated surrounded by alteration zones within serpentinites of dunitic/harzburgitic com-

positions. The massive ore contains more than 90% chromite with chlorite and highly serpentinised olivine. Nodular bodies consist of rounded chromite in chlorite groundmass with magnesite grains and contains 30-90% chromian spinel, as in the brecciated ore. Xenomorphic sulphide grains are found in all types. Major and trace element bulk-rock compositions are very similar to those from GJSM. Chromite textures also show two generations with additional high Al chromite Ia in some grains. Millerite, godlevskite, polydymite and carrolite are occasionally found in these chromitites (Wojtulek et al., 2016).

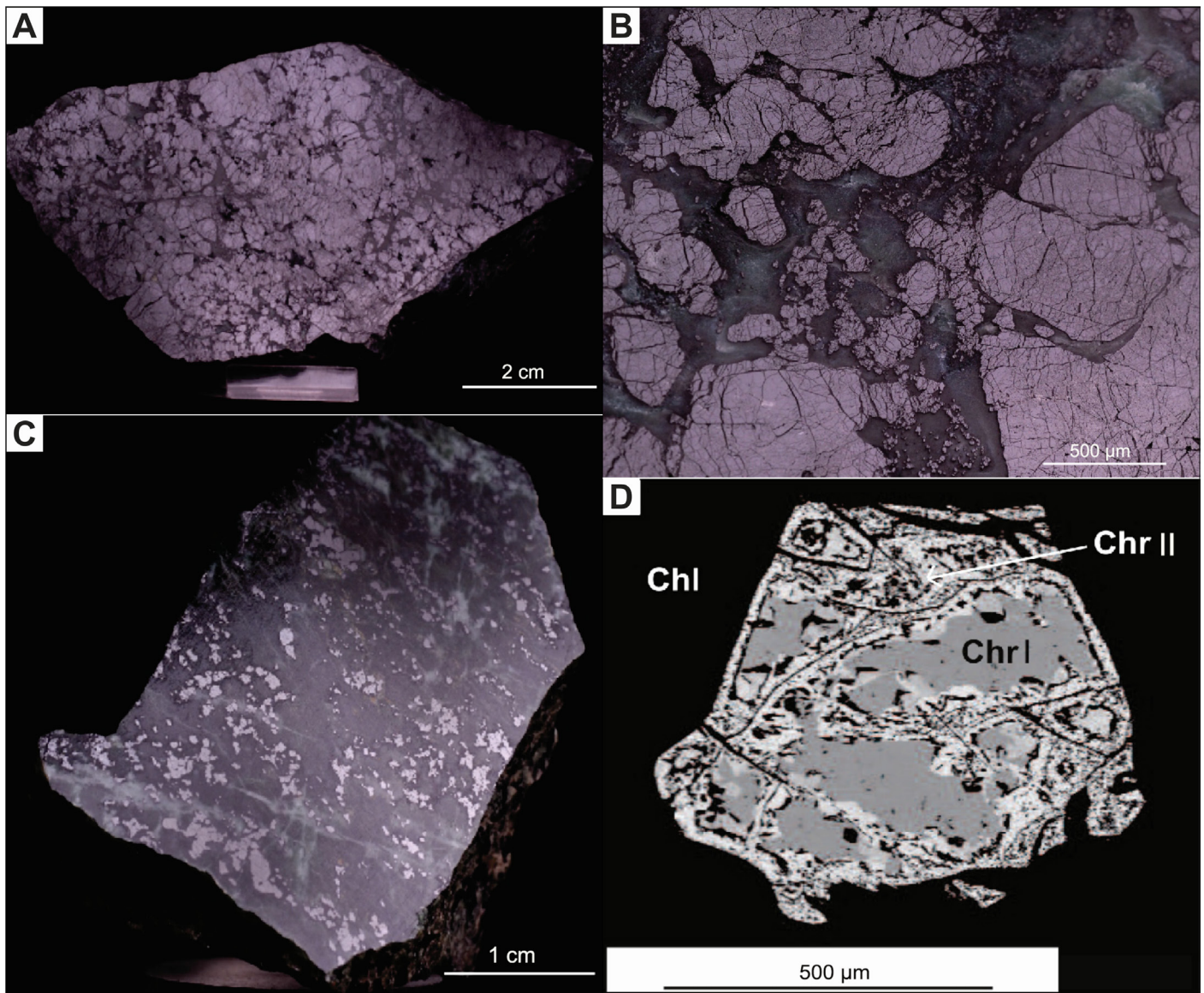


Figure 2: Mode of occurrence and textures of chromitites. A: Massive; B: nodular-brecciated; C: Disseminated; D: Chromite generations, Chromite I and II. (Modified from Wojtulek et al., 2016).

Mechanisms of formation of chromitites

Chromitites from the harzburgites in GJSM and BBM show many similarities and their nodular and podiform textures record igneous crystallization, suggesting that both units crystallized from similar parent melts under similar conditions. They were formed in the first several hundred meters beneath the Paleo-Moho, through the precipitation of chromite from melt migrating in dunite channels in the harzburgitic part of the sub-Moho ophiolite section (Wojtulek et al., 2016). Film-like channels are formed in the dunite-rich parts of the peridotites by melt infiltration and/or crack propagation, resulting in an interconnected 3-D network that produces chromitites when basaltic melts of different provenance and degrees of fractionation mix. Different melt/rock ratios and temperature contrasts between melts and host rock will determine the size, type and structure of the resulting chromitite body (figure 3) (González-Jiménez et al., 2014).

PGE-poor chromitites are related to MOR or supra-subduction zone settings and the low PGE content and Cr# of the chromite in the Lower Silesian chromitites correspond to the Moho Transition Zone (MTZ). Melts migrating through the MTZ form by decompression melting of mantle peridotites and have MOR or arc basalt composition. Moreover, the low TiO₂ content and the Al-rich chromites found in GJSM and BBM are also typical for MORB or arc basalts, which are considered as possible tectonic settings for these chromitites. However, it has been argued that MOR do not produce podiform chromitites, leading to the conclusion that the Lower Silesian chromitites formed in an arc setting, in a supra-subduction zone (Wojtulek et al., 2016).

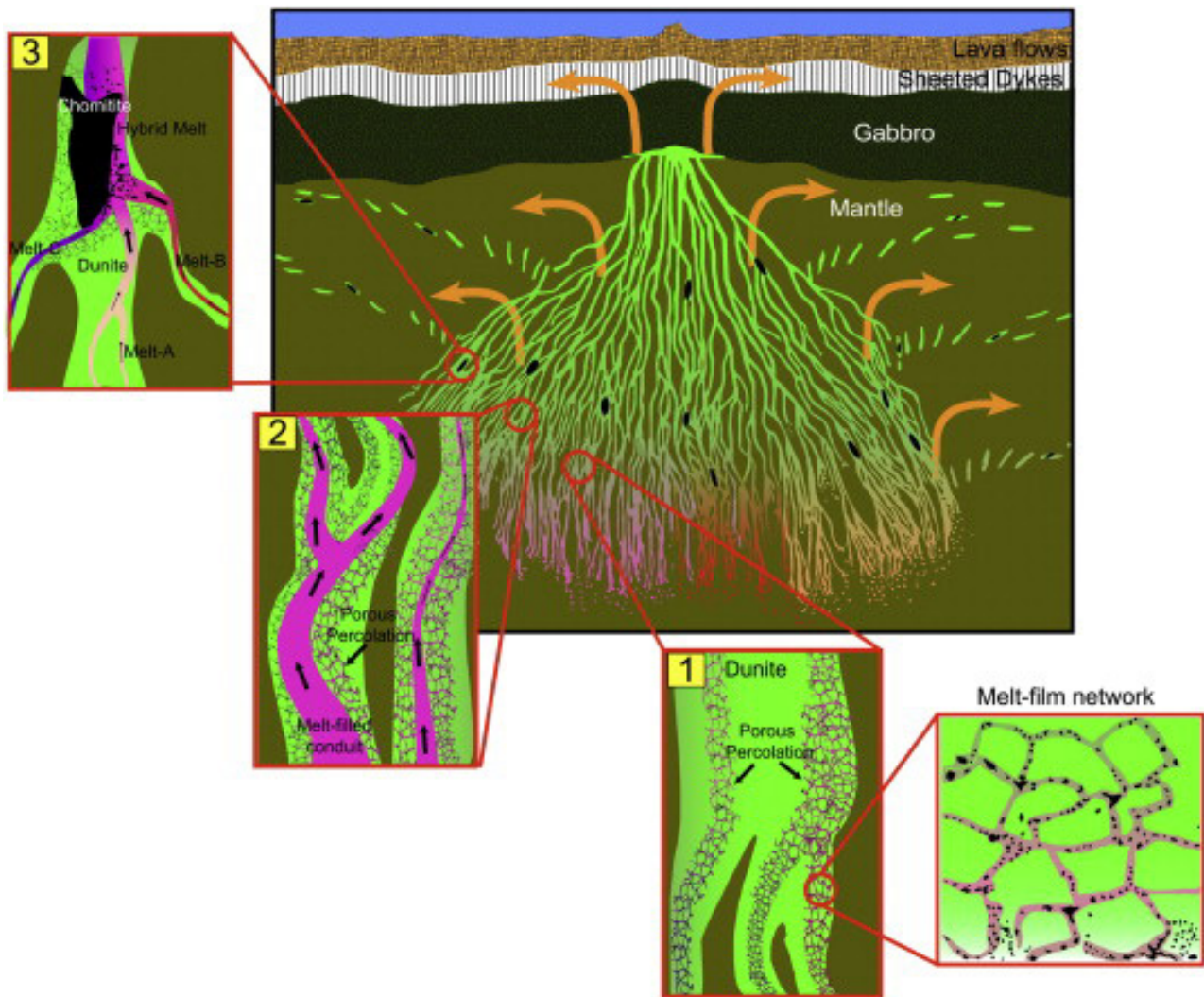


Figure 3: Formation of chromitites in ophiolitic sequences through crystallization from melts ascending in dunite channels from different sources in the upper mantle. 1: Porous percolation through a melt-film network where chromite crystallizes in the zone of intersection due to mixing of basaltic melts; 2: Focused flow produces filled channels allowing isolation and rapid ascent of melts; 3: Mixing of chemically different isolated melts produces large volumes of chromitite (González-Jiménez et al., 2014).

References

- González-Jiménez, J. M., Griffin, W. L., Proenza, J. A., Gervilla, F., O'Reilly, S. Y., Akbulut, M., Pearson, N. J., and Arai, S. (2014): Chromitites in ophiolites: How, where, when, why? Part II. The crystallization of chromitites. *Lithos* 189, 140-158.
- Kryza, R., and Pin, C., (2010): The Central-Sudetic ophiolites (SW Poland): Petrogenetic issues, geochronology and palaeotectonic implications. *Gondwana Research* 17, 292–305.
- Wojtulek, P. M., Puziewicz, J., Ntaflou, T., and Bukala, M. (2016): Podiform chromitites from the Variscan ophiolite serpentinites of Lower Silesia (SW Poland) – petrologic and tectonic setting implications. *Geological Quarterly* 60, 56–66.

intracratonic extensional basins or Carboniferous sandstones and marls (Figure 1; Vaughan et al., 1989). Sea level variations and repeated evaporation of the Zechstein Sea covered the Kupferschiefer black shale with cyclically deposited sequences of limestone and evaporites, mainly halite and anhydrite (Speczik, 1995). Sulfides are hosted within the thin Kupferschiefer layer as well as within overlying dolomitic limestones and underlying red bed sediments. Economic metal accumulations are always associated with irregular and barren hematite alteration zones (*Rote Fäule*). In general, there is a lateral and vertical zonation of sulfides from lower copper-rich to upper lead- and zinc-rich layers and decreasing Cu-grades with distance from zones of *Rote Fäule* (Freese & Jung, 1965).

However, mineralization only occurs locally, and the major part of the Kupferschiefer horizon is essentially barren. This reflects the importance of paleogeographical and structural controls for ore formation. Economic deposits within the Kupferschiefer are associated with paleohighs, shear and fault zones, which were fostering active subsidence. The lower Silesian copper district is thereby regarded to have been formed under euxinic conditions in a deep shelf (Speczik, 1995). Extensional tectonics related to the Variscan evolution in Central Europe caused anomalous elevated geothermal gradients that affected the Kupferschiefer horizon and underlying rocks. Fluid inclusion studies and vitrinite reflectance measurements indicate heat anomalies related to major fracture zones that are spatially proximal to the Kupferschiefer ore deposits (Speczik, 1988).

Basin-scale fluid flow

Generally, it is well accepted that hydrothermal fluids circulated along fractures within the sedimentary sequence and are responsible for metal transport. However, the main fluid flow mechanism is still debated. Jowett (1986) proposed a circulation of highly saline fluids within a closed system driven by elevated heat flow due to rifting during Triassic times. Another model incorporates dewatering by compaction causing rapid fluid expulsion from Rotliegende and Upper Carboniferous sequences (Cathles et al., 1993). A third possibility includes the presence of a thermal anomaly within the lower crust, which triggered ascent of deep basement fluids along a fracture network (Blundell et al., 2003). The main differences between these models are the velocity of fluid flow, the required amount of brine with a specific minimum concentration of copper, and the time required to form the ore deposits.

Ore formation conditions

Despite its name, the Kupferschiefer contains ten times more average concentrations of Pb and Zn than of Cu, with large areas containing even less than average base metal concentrations relative to normal shales (Vaughan et al., 1989). Economic metal accumulations are zoned and associated with sulfide-deficient oxidized zones (*Rote Fäule*), which are regarded as upflow zones of hydrothermal fluids causing a vertical and lateral mineral zonation (Oszczepalski, 1994). Copper-grades are thereby highest close to these zones whereas lead and zinc concentrations increase with distance. The outermost zones are pyrite-rich and continue laterally into barren rocks. Locally, AUPGE concentrations can be significantly elevated close to zones of *Rote Fäule*. The main sulfides chalcocite, covellite, digenite, chalcopyrite, bornite, galena, and sphalerite occur as fine-grained disseminations, cementations, veinlets, and replacements (Figure 2) within the Kupferschiefer and transgressive into overlying dolomitic limestones and underlying Permian red bed or Carboniferous marl sequences (Figure 3; Alderton et al., 2016).

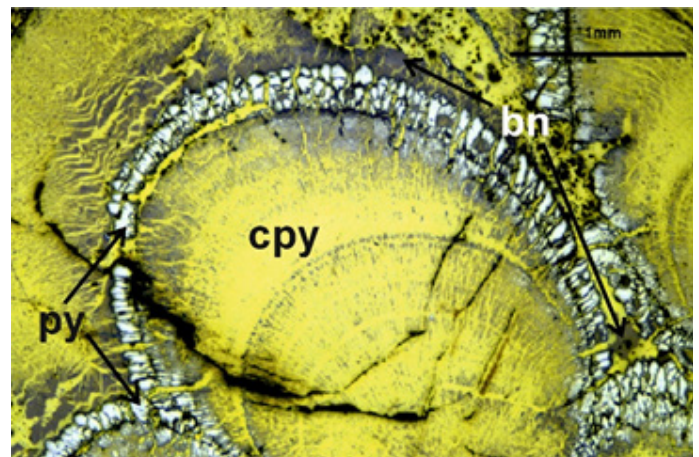


Figure 2: Massive copper ore of concentrically banded chalcopyrite (cpy), pyrite (py), and bornite (bn) under reflected light (modified from Alderton et al., 2016).

The metal source is not well constrained but most investigators consider the underlying lithologies, either the red bed volcanic-sedimentary sequences or the Carboniferous limestones, as principal metal sources. Fluids that have leached metals from these source rocks were probably derived from the Rotliegende sequences either during sedimentation, diagenesis, or epigenetic by intraformational solutions (Speczik, 1995). The long duration of the mineralizing processes (260 to 150 Ma) indicates polycyclic or multi-stage ore formation consistent with continued burial and dewatering of sediments (Alderton et al., 2016).

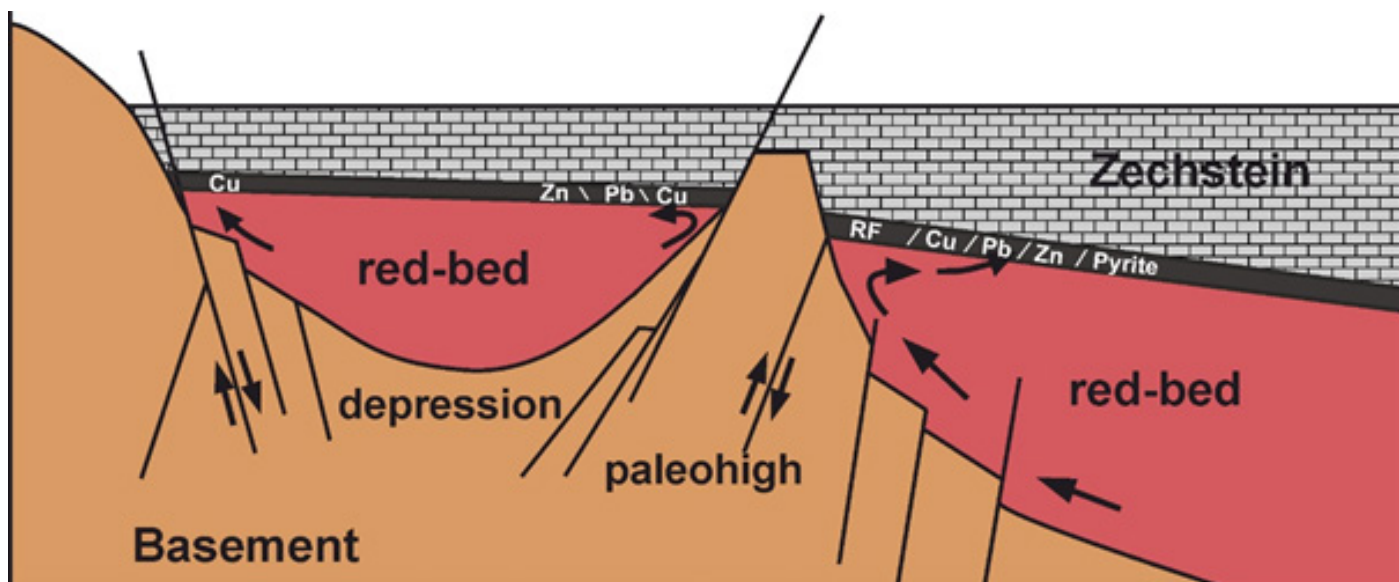


Figure 3: Schematic model illustrating the formation of ore-grade Kupferschiefer (modified from Speczik, 1995).

Fluid inclusion studies indicated that fluids of low to medium salinity and temperatures between 150 and 300 °C were responsible for metal transport (Speczik & Kozłowski, 1987). Circulation of these brines along fractures zones adjacent to paleohighs was thereby probably driven by thermal anomalies associated with active rifting (Blundell et al., 2003). Vertical fluid flow changed to lateral movement along the relatively impermeable Kupferschiefer horizon (Figure 3) causing chemical and physical changes of the hydrothermal fluid. The oxidized and metal-bearing fluids were reduced by converting primary pyrite to hematite (Rote Fäule zones) and oxidization of organic material within the Kupferschiefer producing H_2S . The availability of reduced sulfur led to the precipitation of sulfide minerals. An alternative theory involves mixing of two different brines, a lower high-temperature rather low salinity metal-bearing brine and an upper low-temperature, high salinity SO_4^{2-} brine (Kucha & Pawlikowski, 1986). Bacterial sulfate reduction would have produced the required amounts of reduced sulfides.

Due to the uncertainties in mineralization ages, metal sources, fluid flow and transport, as well as metal precipitation mechanisms, a simple model cannot explain the origin of the Kupferschiefer deposits. However, the specific geotectonic development of Central Europe resulting in the fault-controlled sedimentation of possible source rocks and providing pathways for migrating fluids along paleohighs is key to the formation of the Kupferschiefer deposits in southwest Poland (Speczik, 1995). The complexity of these deposits might be due to several mineralization stages from early syn- to later dia- and epigenetic events of fluid flow and base metal contribution from different source lithologies depending on the regional geology.

The deposits of the Lubin ore field

The Lubin copper ore field in southwestern Poland was the source for the world's sixth largest refined copper supplier, and the third largest source of silver in 2005. The Lubin-Sieroszowice mining district is a strata-bound ore deposit that lies near the Lower to Upper Permian boundary (Wodzicki, 1994). It transgresses the Werra dolomite, the Kupferschiefer organic-rich shale and the Weissliegende sandstone, which overlie barren Rotliegende sandstone (Figure 4).

The fluids are likely to stem from the Early Permian sedimentary basin. There, also volcanic rocks can be found, which are the likely source of the metals, and the nearby Kupferschiefer could be the source of most of the reduced sulphur. The region of upwelling is marked by the Rote Fäule facies penetrating to the level of the Kupferschiefer. Hydrothermal fluids responsible for the "typical" mineralization flowed through the Rotliegende where they equilibrated with feldspar, clays, hematite and anhydrite. The fluids were thus near neutral (pH = 6.3), oxidizing and saturated with respect to anhydrite. These fluids interacted either directly or indirectly with organic matter in the lower Zechstein rocks.

The ore deposits of the Lubin-Sieroszowice district have had a long and complex history of mineralization, which included a synsedimentary or early diagenetic stage, three late diagenetic stages and a tectonic stage. Rifting and lithospheric thinning associated with the opening of the Tethysocean occurred in the area of the Sudetes during the Triassic and Early Jurassic (Ziegler, 1982). Thermal anomalies produced by this event may have played a role in the minerali-

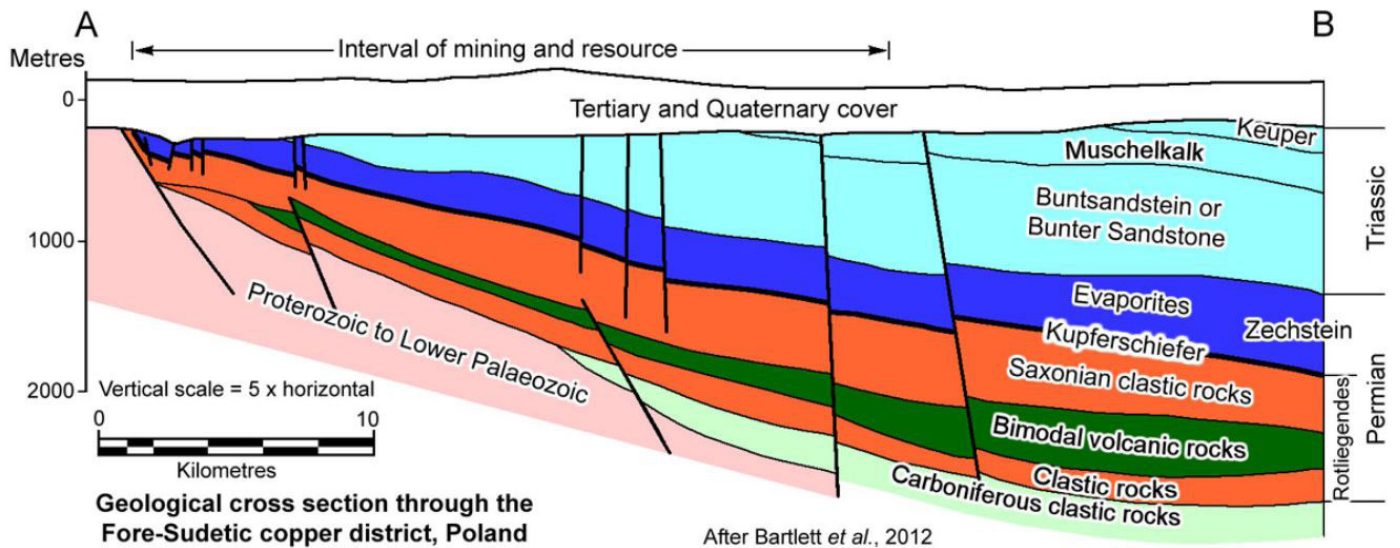


Figure 4: Geologic profile of the Lubin ore district from Porter GeoConsultancy (2013, modified from Bartlett et al., 2012).

zing process (Jowett, 1986). Three types of ore deposits are present in the district: peneconcordant ore in the Kupferschiefer and to a lesser extent in the overlying carbonates (Polkowice and Sierszowice mines); peneconcordant ore in the Weissliegende (Rudna and western Lubin mines); and discordant ore that is peripheral to anhydritic zones in the Weissliegende (Rudna and western Lubin mines). Symsedimentary and early diagenetic (Stage 0) and tectonic mineralization (Stage IV) are of no economic importance in the district (Figure 5).

Ore of the Kupferschiefer-type occurs where upwelling, oxidizing, copper-bearing fluids came into direct contact with the organic shale. Here metals precipitated as a result of reduction by organic carbon in the Zechstein rocks. Ore of the Weissliegende-type occurs where the oxidizing, copper-rich fluids came into contact with an earlier, reducing, buffered fluid that was trapped beneath the Kupferschiefer, possibly in structural traps. Here metals were precipitated as a result of reduction by the earlier fluid. Ore of the anhydrite association occurs peripherally to anhydrite bodies in the Weissliegende where descending, reducing, sulphur-rich fluids displaced and reconcentrated earlier copper/silver ore. This only occurs at locations where the Kupferschiefer is missing, and the descending fluid could penetrate from the overlying evaporites to the Weissliegende (Wodzicki, 1994).

MINERALS	STAGES				
	0	I	II	III	IV
base metals	•••••	••			
chalcocite			•••••	•••••	•••••
bornite	•••••		•••••	•	•••••
chalcopyrite	•••••		•••••		••
tennantite			•••••		•••••
pyrite	•••••	•••••	•••••	••	•
galena		•	•••••	•	•
sphalerite		•	•••••	•	•
native Ag			•	•	•
polymetallic			•••••		••
calcite	•••••	•••••			•••••
dolomite		•••••	•••••		•••••
clays	•••••				
anhydrite	•••••	•••••		•••••	•••••
hematite	△△△△	△△	•••••	△	△
tectonism			⌄	⌄	⌄
ore grade			1-50%	1-98%	

Figure 5: Generalized succession of minerals in the Lubin Sierszowice district (Wodzicki et al, 1993).

References

- Alderton, D. H. M., Selby, D., Kucha, H., and Blundell, D.J. (2016): A multistage origin for Kupferschiefer mineralization. *Ore Geol. Rev.* 79, 535-543.
- Blundell, D.J., Karnkowski, P. H., Alderton, D. H. M., Oszczepalski, S., and Kucha, H. (2003): Copper mineralization of the Polish Kupferschiefer: A proposed basement fault-fracture system of fluid flow. *Economic Geology* 98, 1487-1495.
- Freese, G. and Jung, W. (1965): Über die Rotfärbung der Basalschichten des Zechsteins (Rote Fäule) und ihre Beziehungen zum Nebengestein im südöstlichen Harzvorland. *Freiberger Forschungshefte* 193, 9-23.
- Jowett, E.C. (1986): Genesis of Kupferschiefer Cu-Ag deposits by convective flow of Rotliegende brines during Triassic Rifting. *Economic Geology* 81, 1823-1837.

- Kucha, H. and Pawlikowski, M. (1986): Two-brine model of the genesis of strata-bound Zechstein deposits (Kupferschiefer type), Poland. *Mineralium Deposita* 21, 70-80.
- Oszczepalski, S. (1994): Oxidative alteration of the Kupferschiefer in Poland: oxide-sulphide parageneses and implications for ore-forming models. *Geological Quarterly* 38, 651-672.
- Porter GeoConsultancy (2013), accessed 10.06.2018: Kupferschiefer-Zechstein, Lubin, Rudna, Sierszowice, Polkowice, Glogow, Konrad, Lena, Nowy Kosciol. <http://www.portergeo.com.au/database/mineinfo.asp?mineid=mn401>.
- Rahfeld, A., Kleeberg, R., Möckel, R., and Gutzmer, J. (2018): Quantitative mineralogical analysis of European Kupferschiefer ore. *Minerals Engineering* 115, 21-32.
- Sawlowicz, Z. (2013): REE and their relevance to the development of the Kupferschiefer copper deposit in Poland. *Ore Geology Reviews* 55, 176-186.
- Speczik, S. and Kozłowski, A. (1987): Fluid inclusion study of epigenetic veinlets from the Carboniferous rocks off the Fore-Sudetic Monocline (southwest Poland). *Chemical Geology* 61, 287-298.
- Speczik, S. (1988): Relation of Permian base metal occurrences to the Variscan paleogeothermal field of the Fore-Sudetic Monocline (southwestern Poland). In: G. Friedrich & P.M. Herzig (Eds.) *Base metal sulphide deposits in volcanic and sedimentary environments*. SGA Special Publications 6, 12-24.
- Speczik, S. (1995): The Kupferschiefer mineralization of Central Europe: New aspects and major areas of future research. *Ore Geology Reviews* 9, 411-426.
- Vaughan, D. J., Sweeney, M., Friedrich, G., Diedel, R., and Haranczyk, C. (1989): The Kupferschiefer: An overview with an appraisal of the different types of mineralization. *Economic Geology* 84, 1003-1027.
- Wodzicki, A., and Piestrzyński, A. (1994): An ore genetic model for the Lubin—Sierszowice mining district, Poland. *Mineralium Deposita* 29, 30-43.
- Ziegler, P.A. (1982): *Geological atlas of western and central Europe: The Hague, Shell International Petroleum Maatschappij B.V.*, 130p.

The Bełchatów open pit coal mine: geology, current state and future of lignite mining in Poland

Taraneh Roodpeyma

- Bełchatów coal mine has one of the largest coal reserves in Poland, with estimated reserves of 1930 Mt of lignite coal
- Predicted economic resources of Poland in terms of brown coal reached 23451.13 Mt as of the end of 2016
- 52.8 TWh of electricity, one third of the total gross power generated in Poland, is related to lignite-fired power stations

Introduction

Coal forms when dead plant material turns into swamps and peat bogs that are buried by accumulating silt and other sediments, along with tectonic movements. The plant material is transformed into coal seams under high temperatures and pressures over millions of years. The formation of coal began during the Carboniferous Period, ca. 360 to 290 million years ago (World Coal Institute, 2005).

The 'organic maturity' relates to the quality of each coal deposit based on the temperature, pressure, and the time span of formation (maturation). In the first stage, the peat is converted into 'lignite' or 'brown coal'. Lignite is the softest coal and may show various shades of brown. The mentioned circumstances cause further changes in the lignite, transforming it into 'sub-bituminous' coals. The more mature, harder and darker coals are called 'bituminous' or 'hard coals'. In case of even longer maturation, 'anthracite' is formed (World Coal Institute, 2005).

Poland is the second largest coal producer in Europe but is also a main oil and natural gas importer. In 2015, Poland's total primary energy consumption was 3.8 quadrillion Btu (British Thermal Unit). According to the 2016 BP Statistical Review of World Energy, coal amounted to 52% of the consumption, with the remainder consumed as oil (26%), natural gas (16%), and renewable energy sources (5%) (U.S. Energy Information Administration, 2016).

In 2014, Poland was ranked the 9th and 8th place in the world for production of 136.4 Mt and consumption of 137.9 Mt of coal, respectively. This translates into 22% of total coal production and 16% of total coal consumption in Europe. Production and consumption

of lignite were 63.9 Mt and 63.8 Mt, respectively, i.e. ca. 45% of total coal production and consumption. The coal is mainly used for power generation in Poland (U.S. Energy Information Administration, 2016).

The lignite forms single beds, lentils or complexes of beds within other sediments belonging to Paleocene to Upper Miocene periods. The lignite deposits are located mainly in the western, southern and central parts of Poland and the surface of lignite-bearing strata in the Lowland is around 100,000 km² (Figure 1) (Volkmer, 2008).

The Bełchatów lignite coal mine consists of two lignite fields: Bełchatów and Szczerców, with estimated reserves of 1,930 Mt of lignite coal, making it one of the largest coal reserves in Poland. Its production, in

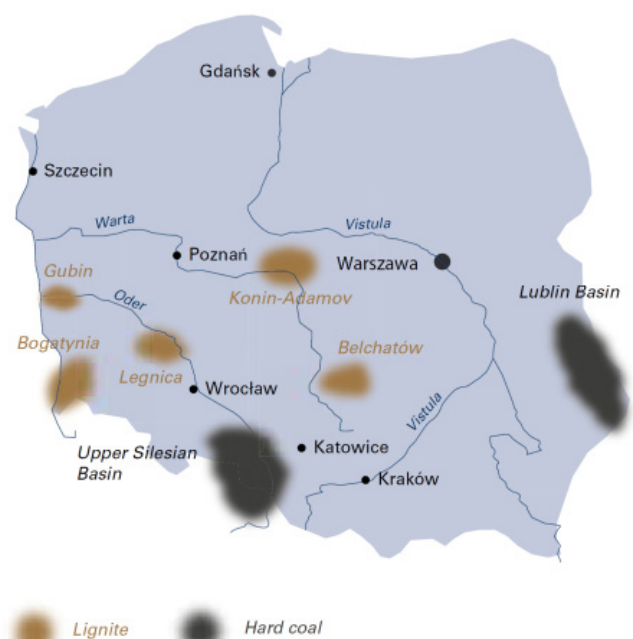


Figure 1: Locations of Polish coal deposits, from Polish Geological Institute (2015).

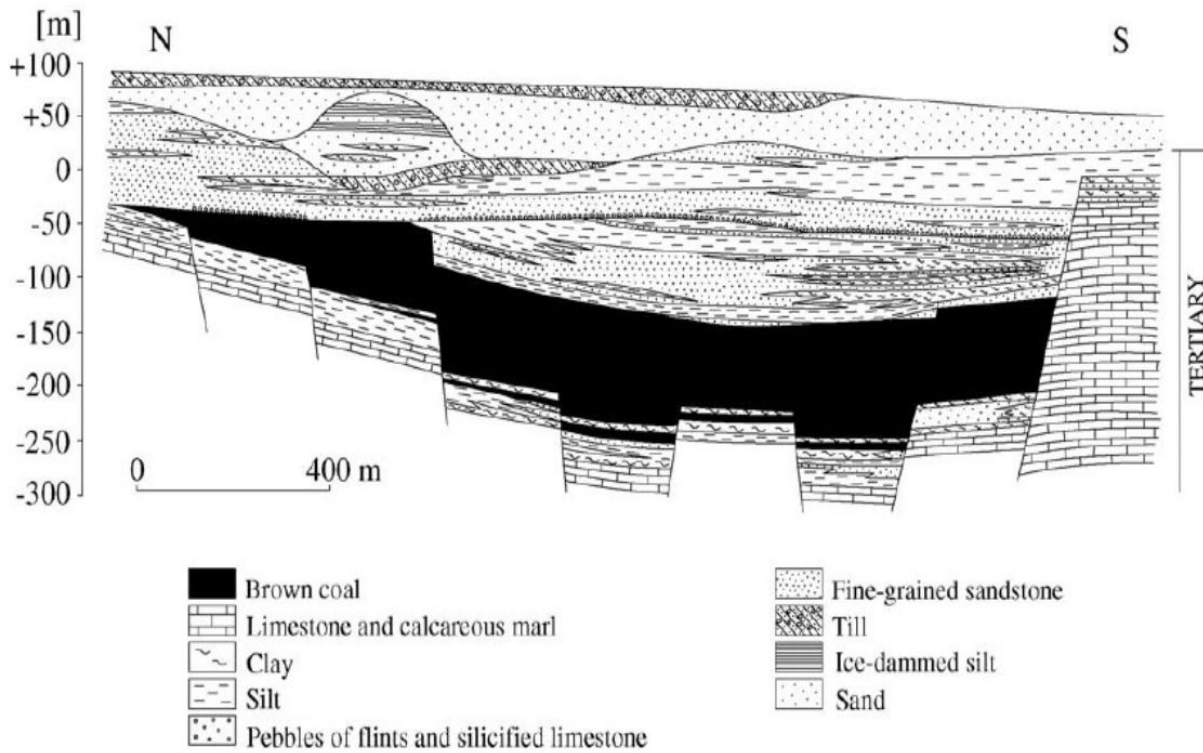


Figure 2: Geologic section of the Belchatów deposit after Ciuk (1970), from Volkmer (2008).

2015, was 42.1 Mt of lignite or 66.7% of Poland's total lignite. It is predicted that the Belchatów mine will remain in operation until 2040. A nearby power plant owned by PGE GiEK, with a capacity of 5,298 MW, uses the lignite output to generate power (31.7 TWh in 2015). Thereby, around 19% of the domestic power consumption is covered. A new power plant went on stream in 2011 (Poltegor, n.d., Loon, 2002).

Geology of the Belchatów lignite basin and the Kleszczów graben

The Belchatów lignite basin is located in an area where Miocene coal occurs in a series of tectonic grabens (Figure 2). These grabens are more than 40 km long and 1.5 to 2.0 km wide (Volkmer, 2008).

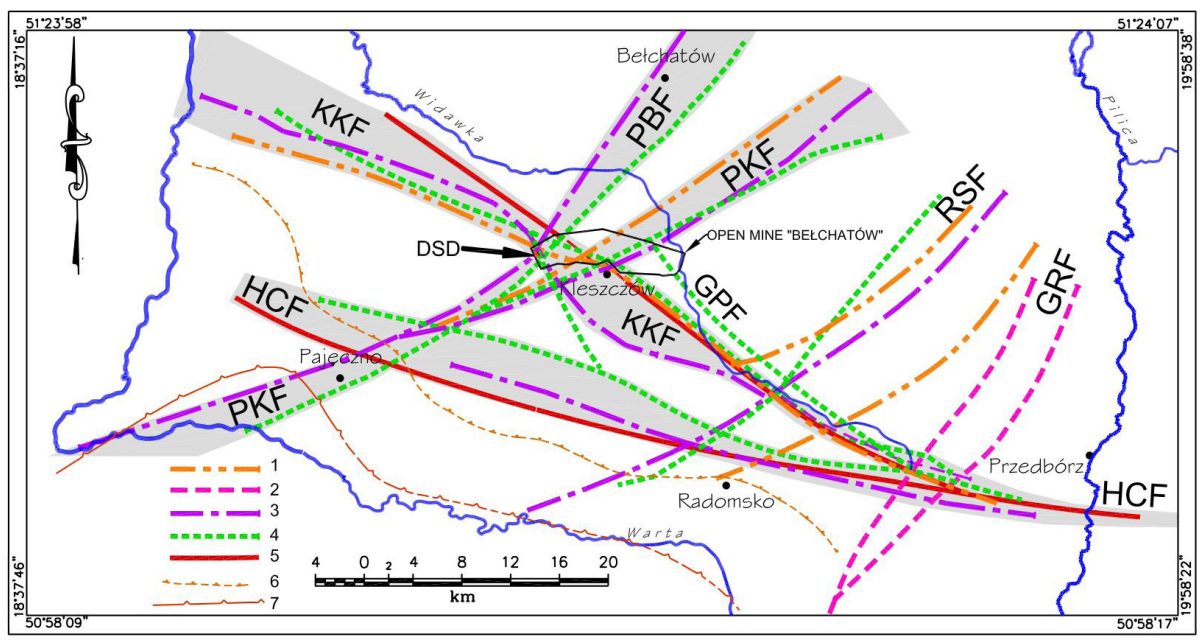


Figure 3: “Main regional faults in the Permian-Mesozoic complex of the Kleszczów Graben area. Based on an analysis of the sediment thickness and the top surface morphology of selected units

(up to Middle Jurassic, inclusive). Notations are: 1) best recorded in Permian complex; 2) best recorded in Early Triassic to Late Triassic complex; 3) best recorded in Middle Triassic to Late Triassic complex; 4) best recorded in Late Triassic to Middle Jurassic complex; 5) recorded in most units of the Permian-Mesozoic complex; 6) limit of the Rotliegend deposits; 7) limit of the Zechstein deposits. Abbreviations are: HCF – Holy Cross Fault; KKF – Kodań-Kleszczów Fault; GPF – Gomunice-Piaski Fault; PKF – Pajęczno-Kleszczów Fault; PBF – Pajęczno-Belchatów Fault; RSF – Radomsko-Sulejów Fault; GRF – Gidle-Ręczno Fault; DSD – Dębina Salt Dome.” From Gotowała and Hałuszczak (2002).

The Kleszczów graben is presumably a result of tensional fracturing and faulting of the anticlinal hinge zones at the transition from the Radomsko elevation to the Łódź depression, during the Early Tertiary. The structural trend is followed by the actual (E–W) graben direction in the Carboniferous (and older) substratum, found in the Mesozoic hard-rock (Figure 3) (Loon, 2002).

The Late Alpine Kleszczów Graben is situated in a zone of intersection with deep-seated, regional dislocations, such as the HCF and the BKF (Figure 3). The formation of the graben resulted from earlier tectonic events: the Early and Middle Alpine, or even Variscan orogeny. The reactivation of these faults trending NW-SE, NE-SW, WSW-ENE and WNW-ENE, during the Tertiary-Quaternary formed the present day structural framework of the Kleszczów Graben and its sedimentary infill (Loon, 2002).

The lake deposits in the Quaternary overburden of the Bełchatów lignite mine in the central part of Poland show glaciolacustrine sedimentation within an active graben. These deposits may have formed also during successive glaciations and are unique in Europe (Figure 4) (Gruszka, 2007).

Lignite Mining: current and future state

There is no free-market price for lignite used in power generation. This is because of its low calorific value, which makes the transport uneconomic over longer distances. The cost of lignite per unit of energy, including transport, are higher than that of hard coal, and lignite-fired power plants are not able to purchase fuel from distant mines. Both producer and consumer co-exist in a captive market, which results in higher prices and less diversity which forces potential consu-

mers to purchase a good or service from a particular supplier (Polish Geological Institute, 2015).

The brown coal resources are calculated to reach a maximum depth of 350 m, with a minimum lignite layer thickness of 3 m and maximum overburden/deposit thickness ratio of 12:1 (Szmałek and Tyminski, n.d.).

In recent years, due to the lower coal prices and higher production costs, the coal mining industry has been negatively influenced by the reduction of domestic output. Although the government is still supporting this industry, they decided to invest in other fuel developments. However, in 2016, several state-owned energy utility companies provided fertile ground, with their investments, to prevent Kompania Węglowa, the European Union's largest coal mining company, from bankruptcy (U.S. Energy Information Administration, 2016).

Poland's lignite mines, with 6500 t per year average productivity in 2015, can keep its annual production output at current levels of around 60 Mt while lignite is estimated to have a significant effect on Poland's energy supply until at least 2030 (Polish Geological Institute, 2015).

In 2017, 61.0 Mt of lignite was produced, which is 1.3% higher than what was produced in 2016. In addition, lignite-fired electricity provided 52.3 TWh of the 169.8 TWh total generation, showing a 30.8% share. Along with the closure of the 600 MW Adamów power plant, part of the Pątnów-Adamów-Konin group, at the beginning of January 2018, the construction of power units 5 and 6 at PGE's Opole power plant, according to a company announcement in November 2017, is 88% completed and also the new 450 MW unit at Turów lignite power plant is progressing well. Finally, in December 2017, after being commissioned,

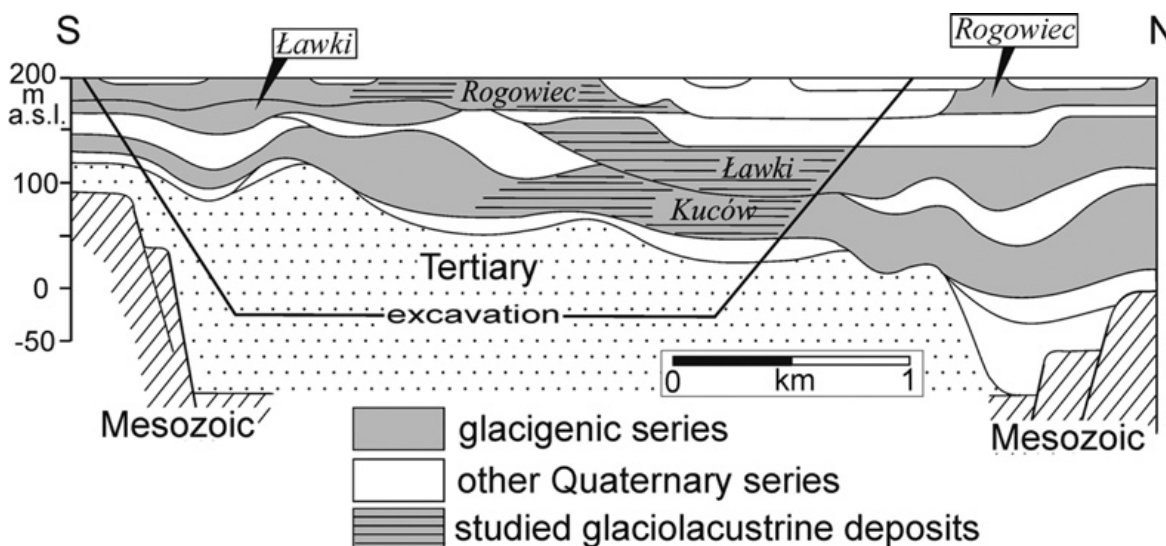


Figure 4: Schematic cross-section through the Kleszczów Graben. Modified after Brodzikowski (1995), from Gruszka (2007).

the 1075 MW Koźienice power plant (achieving an efficiency of 45.6%), allows a carbon emission reduction of about 25% compared with existing coal-fired blocks (Polish Geological Institute, 2015).

The three scenarios for the future of Polish lignite mining, according to the newest Polish energy policy (Project of the Energy Policy of Poland till 2050), are (Widera et al., 2016):

1. The pessimistic scenario: the development of lignite mining activity in Poland is prone to reduction until the year 2045.
2. The realistic scenario: with almost the same amount of lignite output and developing satellite deposits, this development covers a longer period to 2055.
3. The optimistic scenario: extending all currently operating lignite mines' activities by applying new open casts could be predicted. However, as mentioned above, Adamów power plant was shut down at the beginning of January 2018; so this scenario may change .

References

- Gotowała, A. and Hałuszczak, R. (2002): The late alpine structural development of the Kleszczów Graben (central Poland) as a result of reactivation of the pre-existing, regional dislocations. EGU Stephan Mueller Special Publication Series 1, 137-150.
- Loon, A. J. (2002): Soft-sediment deformations in the Kleszczow Graben (central Poland). *Sedimentary Geology* 147, 57-70.
- Polish Geological Institute (2015), accessed 06.06.2018: euracoal.eu.
- Poltegor (n.d.), accessed 06.06.2018: References 1950-2016 - Projekt sp. z.o.o. http://www.poltegor.pl/pliki/references_2016-web.pdf.
- Szamalek, K. and Tyminski, M., for the Polish Geological Institute (n.d.), accessed 06.06.2018: Mineral Resources of Poland. geoportal.pgi.gov.pl.
- U.S. Energy Information Administration (2016), accessed 06.06.2018: www.eia.gov.
- Widera, M., Kasztelewicz, Z., and Ptak, M. (2016): Lignite mining and electricity generation in Poland: The current state and future prospects. *Energy Policy* 92, 151-157.
- World Coal Institute (2005), accessed 06.06.2018: The coal resource: a comprehensive overview of coal. www.worldcoal.org.

Carbonate-hosted Pb-Zn deposits in the Upper Silesia: Geological setting and ore precipitation mechanisms

Thierry Solms

- Pomorzany-Olkusz is classified as a Mississippi-Valley-type (MVT) ore deposit and is part of the Silesia-Cracow Zinc-Lead district.
- The main mineralization consists of sphalerite and galena and is found in the lower Muschelkalk.
- Mineralization styles comprise replacement precipitation, fracture fillings, and cementations.

Geological setting

The most important mineralization occurrences (predominantly sphalerite and galena) are found in the lower Muschelkalk Formation, a lithological unit which originates from the deposition of carbonates in a relatively shallow ocean basin which covered a big part of Central Europe during the Anisian (243 to 235 Ma). The pre-Mesozoic basement in the eastern parts of the Silesia-Cracow district consists of sequences of flysch sediments (Cambrian and Silurian age, up to 12 km thick), which were folded and metamorphosed during the Caledonian orogeny. Above this basement, Devonian and Carboniferous sandstones and carbonates are found. The western parts of the district belong to the Upper Silesian coal basin, where the Precambrian basement is overlain by sandstones, carbonates and flysch of Cambrian to Lower Carboniferous ages, and coal-bearing Carboniferous molasse sediments. These lithologies were intensely folded during the Variscan orogeny. Thrust faults and normal faults are found in the western and eastern part of the Silesian basin, respectively. In the Triassic, marine transgression led to the formation of seawater basins with carbonate platforms, interspersed with islands of Paleozoic basement (Leach et al., 1996).

In these basins, the following characteristic lithologies of the Germanic Triassic were deposited: Buntsandstein (red sandstones, evaporites and dolostones), Muschelkalk (mostly limestone, minor dolostone, clays and sandstones) and Keuper (non-marine clays). Tectonic activity related to the (early) Alpine orogeny led to uplift in the region and periods of marine regression, which led to karstification and erosion between the Upper Triassic and Middle Jurassic (Glažek, 1989). Palynological and petrological studies performed on organic matter in the karst systems of the Silesia-Cracow district suggest that an earlier period of karstification occurred in the Middle Triassic just after the carbonate precipitation during the Anisian (ca. 245 Ma). The analyzed organic matter is thought

to originate from terrestrial biomass and was found to be preserved very well, indicating low oxidation potential, e.g. caused by high sedimentation rates in the karst systems (Rybicki et al., 2017).

This first pulse of tectonic activity related to the Alpine orogen led to the formation of low-amplitude folds and the reactivation of pre-Mesozoic basement faults, which produced widespread faulting and fracturing with small displacements. Sedimentation started again in the Middle Jurassic and went on until the Cretaceous, leading to the deposition of carbonates and sandstones. A second, more intense pulse of Alpine tectonics produced widespread faults and fractures and the Silesia-Cracow monocline. A third, Late Alpine tectonic pulse is related to the formation of the Carpathian foredeep and foldbelt in the south of the district, which reactivated earlier Variscan and Early Alpine fault systems. This pulse led to strike-slip faults with displacement of several kilometers and normal faults, producing a dense fault network. This tectonic pulse is represented on the district-scale by horst and graben blocks, which are host to some of the most important ore bodies in the district, possibly due to the steep faults that probably acted as pathways for ore-bearing fluids (Leach et al., 1996). The presence of steep faults as main fluid pathways distinguishes the Silesia-Cracow district from “typical” MVT deposits where the elevation gradients are generally thought to be small. This has implications for the underlying mechanisms driving the transport of ore-bearing fluids on regional scale and hence for the genetic model of the Silesia-Cracow deposits.

Mineralization mechanisms

Most of the important mineralization zones are found in the Lower Muschelkalk formation, in the so-called „ore-bearing dolostone“, a dolomitized carbonate. The ore bodies generally show a tabular geometry with carbonate replacement as the main sulfide precipitation mechanism. This kind of mineralization leads to

the preservation of the initial rock texture, resulting in bands of sphalerite and galena as replacement for internal layers of the dolostone. When sulfide-rich fluids and metal-bearing brines interact, sulfides precipitate and H^+ is produced, which will dissolve the carbonate host rock making space for the precipitating minerals. If this reaction occurs, one mole of carbonate is dissolved per mole of sulfide precipitated. If the sulfur in the brine is present as sulfate, a reducing agent (e.g. reduced C) must be present. The dissolution efficiency is then mainly governed by the stoichiometry of the reductant (Corbella et al., 2004). However, sulfur isotope studies showed that the range of isotope values is much larger than would be expected only from the reduction of sulfate by organic matter.

Besides replacement precipitation, open space fillings, fracture fillings and cementation by precipitated sulfides occur. Age constraints from the faults which are being crosscut by the ore bodies indicate that the mineralization event(s) did not occur before the Late Jurassic. In the Pomorzany-Olkusz ore body, the mineralizations were subject to Miocene (< 23 Ma) faulting (Late Alpine tectonics), which puts another temporal constraint on the mineralization events.

Fluid inclusion Rb-Sr dating applied to sphalerite from the district indicate that the main mineralization event occurred in the Lower Cretaceous (135 ± 4 Ma), with fluid temperatures assumed to be between

70 and 160 °C (Heijlen et al., 2003). Conclusions from this potential age of the mineralization should be drawn with care, as these Rb/Sr signatures are by some believed to be subject to contamination by clays, carbonates and volcanic tuffs. Paleomagnetic dating, a method more commonly applied to MVT mineralizations indicates Tertiary ages for the Upper Silesian ore bodies. This Tertiary age agrees well with the gravity-driven fluid transport model related to the Alpine orogenesis and the formation of the Carpathian fore-belt (Symons et al., 1995).

Assuming that the gravity-driven fluid flow model for the ore bodies is correct, a long-range pathway for the metal-bearing fluids along distinct geological formations probably occurred. Supporting this theory is the data of Pb isotopes measured on galena, which shows very homogeneous values. Upper Carboniferous sediments are potential candidates for the introduction of Pb (and potentially Zn) into the migrating fluids. Trends from sulfur isotope data contrasts those of Pb isotope data, showing great heterogeneity in the isotope signature within the district, which indicates the interaction of different potential sources of reduced sulfur required for sulfide precipitation (e.g. reduction of sulfate from evaporites by nearby coal beds, biogenic reduction of sulfur in or near the location of the ore bodies, or local reduction by organic matter). The potential for a range of different S isotopes is amplified by the vertical faults which worked as fluid conduits and which allowed the mixing of fluids from geological formations of varying ages and different chemical compositions. It is thought that the saline formation water which potentially originated from the evaporation of seawater (Permian and Triassic sediment formations) and meteoric waters had finally mixed to relatively rapidly precipitate fine-grained sulfides. (Leach et al., 1996).

The relation between the karst systems and the ore precipitation is discussed ambiguously: While some researchers state that the system was created simultaneously with the deposition of ore, others think that a paleokarst system already existed when the ore fluids entered the system and that it was potentially enlarged by those fluids. Evidence for the latter comes from the occurrence of mineralized, internal sediments in karst caves within the main ore bodies, and the absence of such sediments in distal, non-mineralized parts of the karst systems (Leach et al., 1996).

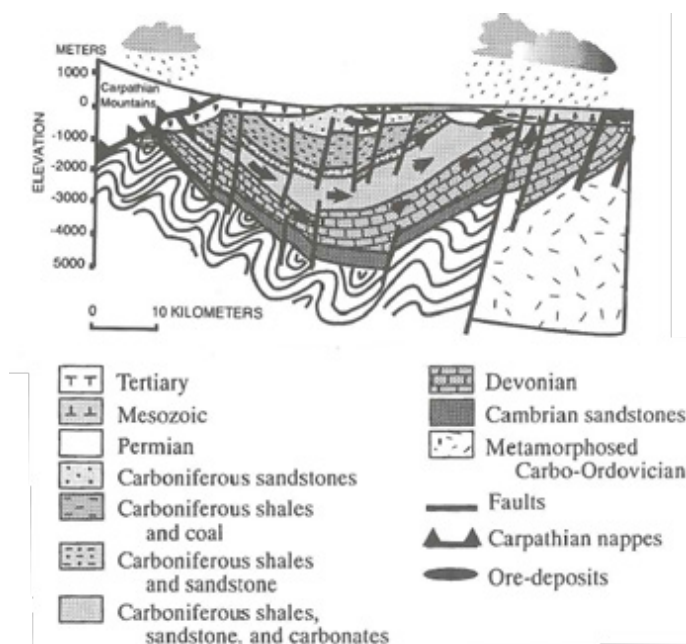


Figure 1: Proposed fluid transport on regional scale for the Silesia-Cracow Zinc-Lead district, showing the gravitationally-driven fluid transport. Ascent into the karst-systems would occur in areas of intense fracturing. From Leach et al. (1996).

References

Corbella, M., Ayora, C., and Cardellach, E. (2004): Hydrothermal mixing, carbonate dissolution and sulfide precipitation in Mississippi Valley-type deposits. *Mineralium Deposita* 39, 344–357.

Glazek, J. (1989): Paleokarst of Poland. *Developments in Earth Surface Processes* 1, 77–105.

Heijlen, W., Muchez, P., Banks, D. A., Schneider, J., Kucha, H., and Keppens, E. (2003): Carbonate-hosted Zn-Pb deposits in Upper Silesia, Poland: Origin and evolution of mineralizing fluids and constraints on genetic models. *Economic Geology* 98, 911–932.

Leach, D. L., Viets, J. G., Kozłowski, A., and Kibitlewski, S. (1996): Geology, geochemistry and genesis of the Silesia-Cracow zinc-lead district, Southern Poland. *Society of Economic Geologists, SEG Special Publications* 4, 144–170.

Rybicki, M., Marynowski, L., Stukins, S., and Nejbort, K. (2017): Age and origin of the well-preserved organic matter in internal sediments from the silesian-cracow lead-zinc deposits, southern Poland. *Economic Geology* 112, 775–798.

Symons, D. T. A., Sangster, D. F., and Leach, D.L. (1995): A Tertiary age from paleomagnetism for mississippi valley-type zinc-lead mineralization in Upper Silesia, Poland. *Economic Geology* 90, 782-794.

Pomorzany-Olkusz mines and the Silesia-Cracow District: fluid inclusions and insight into ore deposition processes

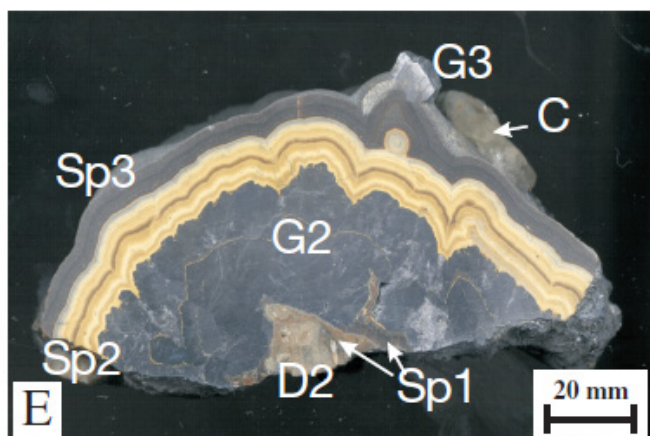
Leslie Logan

- Mineralization is related to the cooling of a fluid (max. 155 °C) originating from evaporating seawater, reaction with the wall rock, deep ascending fluids, and mixing with meteoric water.
- Three fluid populations in sphalerite: low-salinity high-temperature, high-salinity moderate-high temperature, low-salinity low-moderate temperature

Introduction

Ore deposits in the Silesia-Cracow mining district are classified as carbonate-hosted epithermal type Pb-Zn deposits (Kozłowski, 1995) and have also been argued to be Mississippi Valley Type deposits (Heijlen et al., 2003). Economic minerals in the district include py-

rite, marcasite, sphalerite, and galena (for paragenetic sequence see Figure 1). They are primarily located in dolomitized limestone of the lower Muschelkalk formation occurring as horizontal lenticular replacement bodies of varying thickness. Other ore mineralization also occurs in similar limestone units, as fissure and cavity filling, as cement in collapse breccias, and as brecciated ore bodies (Kozłowski, 1995).



Fluid inclusions

Insight about mechanisms of metal precipitation can often be illuminated by conducting well-constrained fluid inclusion studies. In particular is the study by Kozłowski (1995), who used fluid inclusions in early-stage sphalerite to obtain information about the original ore-forming fluids of the system. Sphalerite in the studied sample contains distinct textural differences that reflect the changes in crystal growth rate:

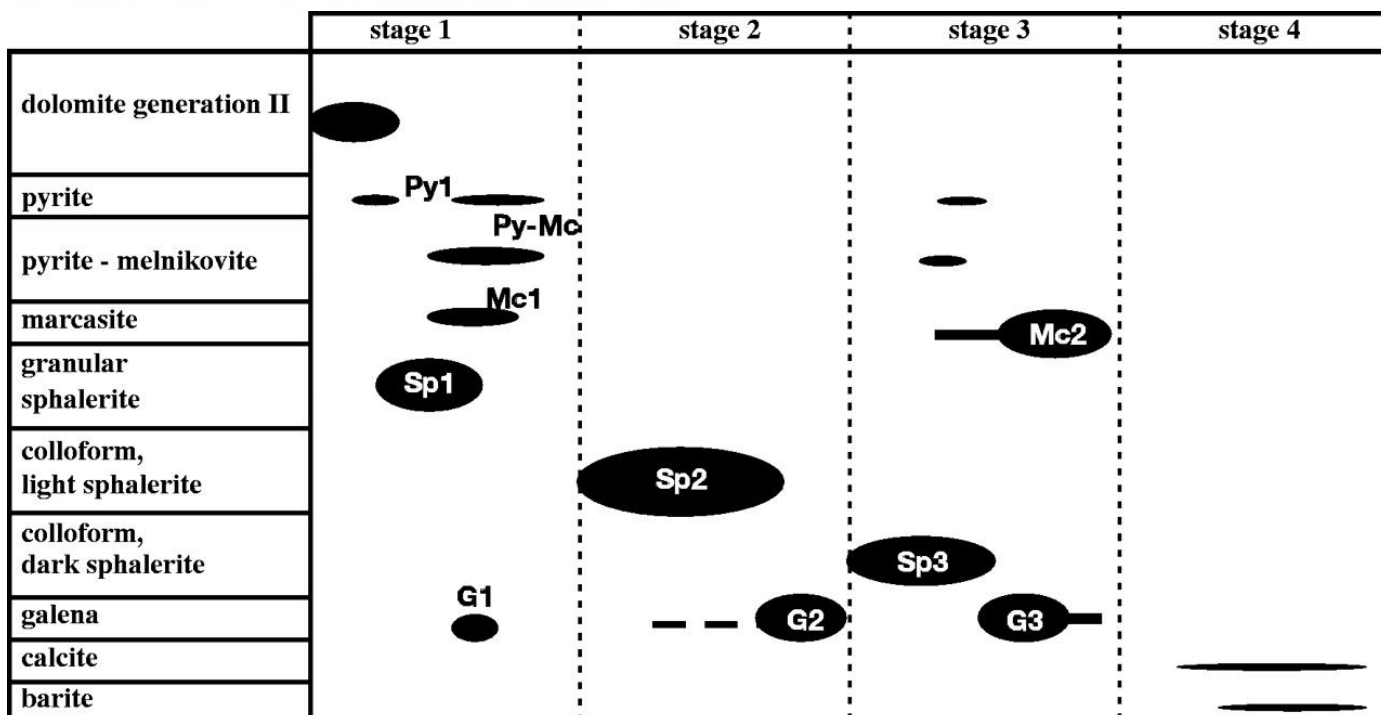


Figure 1: Generalized paragenetic sequence of the Trzebieńka-Pomorzany Zn-Pb ores, Upper Silesia and banded ore from Upper Silesia, showing the different paragenetic stages (Heijlen et al., 2003).

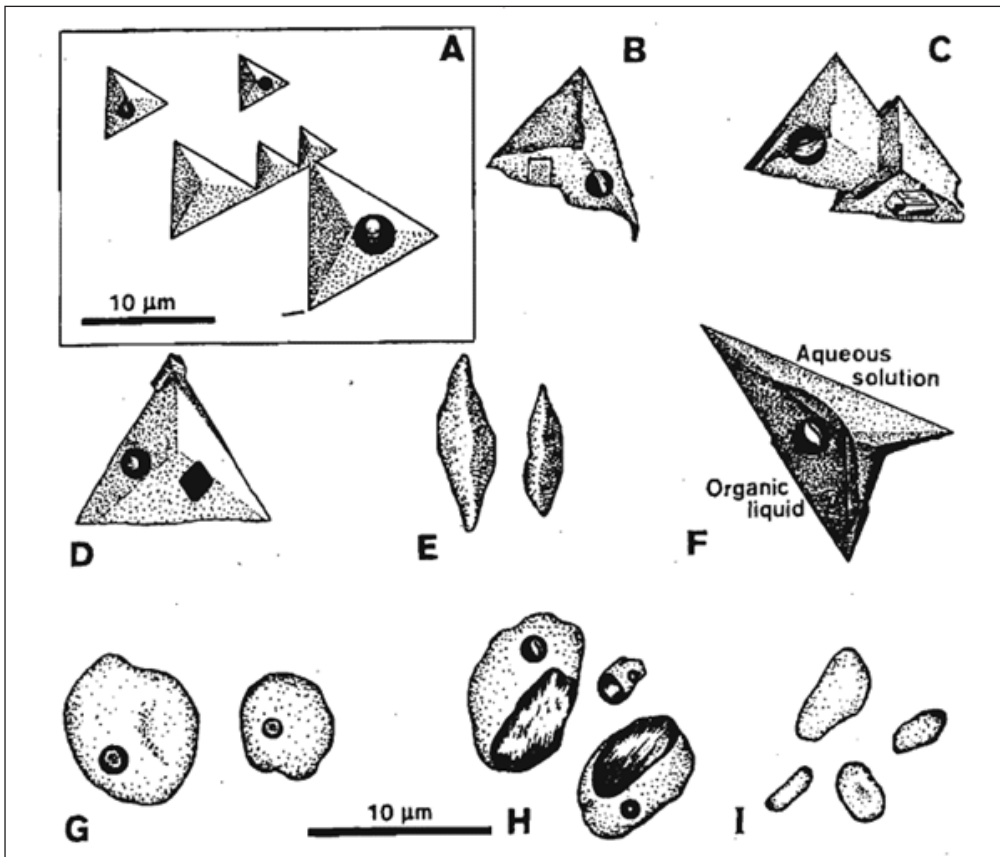


Figure 2: A - tetrahedral aqueous inclusions; B - aqueous solution, gas bubble, halite daughter crystal; C - Aqueous inclusion with gas bubble and trapped carbonate mineral (dolomite?); D - Aqueous inclusion with a gas bubble and trapped opaque mineral; E - One-phase aqueous liquid inclusions; F - Inclusion bearing aqueous and organic liquids and gas bubble; G - Inclusions with organic liquid and gas bubble; H - Inclusions bearing organic liquid, gas bubbles, and organic solid phases; I - One-phase inclusions filled with organic liquid (Kozłowski, 1995).

fibrous (rapid, often in contact with the cooler host dolomite), and granular (slow). Up to nine varieties of primary and secondary fluid inclusions occur in both textures of sphalerite (Figure 2). Microthermometric salinity and homogenization temperatures (T_h) from two- and three-phase primary and secondary inclusions indicate three populations of fluids: a low-salinity high-temperature fluid, a high-salinity moderate-high temperature fluid, and a low-salinity low-moderate temperature fluid (Figure 3). Only two 3-phase inclusions were found by the authors and therefore do not represent a significant part of the population in these results. The authors tentatively interpret that these populations represent deep ascending fluids, saline formation brines, and descending meteoric water, respectively, and suggest they have been strongly mixed. The interpretation of the thermal evolution of fluids in the sphalerite can be seen in Figure 4. This sample contains inclusions with relatively stable salinity measurements, allowing for isolation of temperature data and thermal reconstruction. Temperature variations indicate that a hot parental fluid entered the fissure and cooled in contact with the dolomite wall rock, and continued to pulse through forming fibrous dolomite to a maximum temperature of 155°C. The remaining ZnS in solution contributed to the slow granular sphalerite growth, cooling due to heat outflow rather than as a result of mixing with a cooler solution (no salinity change).

Heijlen et al. (2003) conducted another study on fluid inclusions from the district and obtained elemental ion concentrations using bulk crush-leach methods and analysis by ion chromatography as well as flame emission spectrometry. They analyzed a variety of stages in the paragenetic sequence: dolomite generation I and II, early and late sphalerite (Sp1, Sp3), main-stage

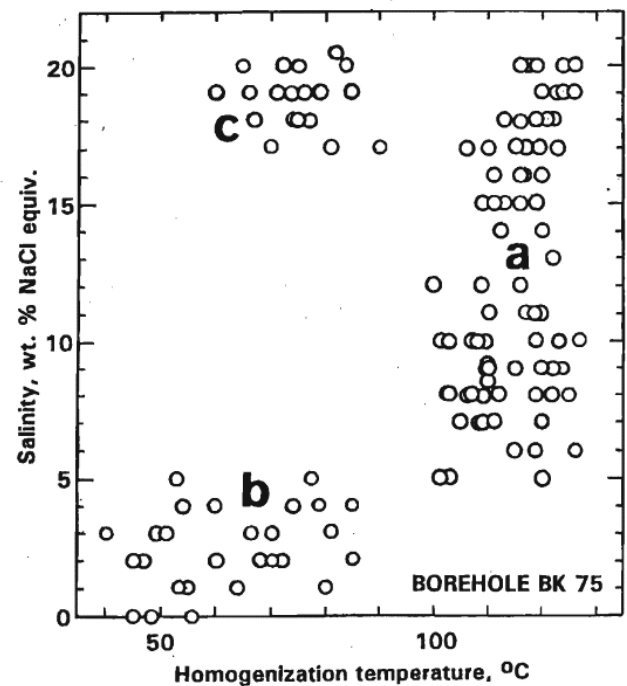


Figure 3: Salinities of inclusion fluids in sphalerite versus homogenization temperatures; (a) ascending solutions, (b) meteoric waters, (c) formation brines (Kozłowski, 1995).

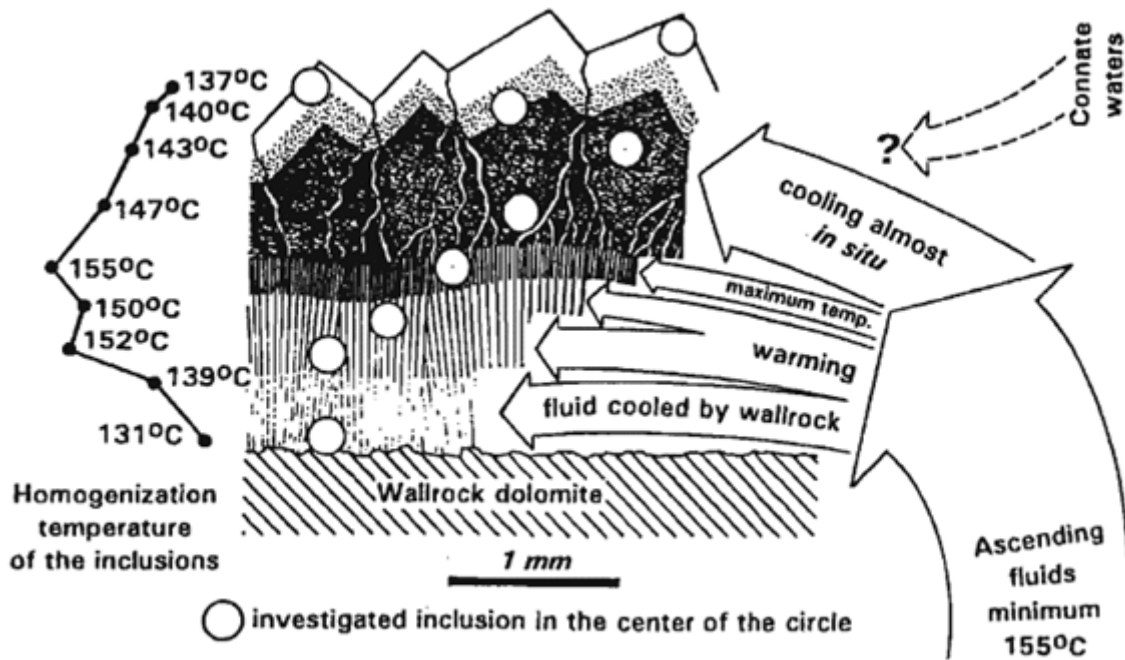


Figure 4: Thermal evolution of fluid precipitating sphalerite in a thin fissure in dolomite showing the changes in textures with temperature and the interpretation of homogenization temperatures from fluid inclusions in the different zones (Kozłowski, 1995).

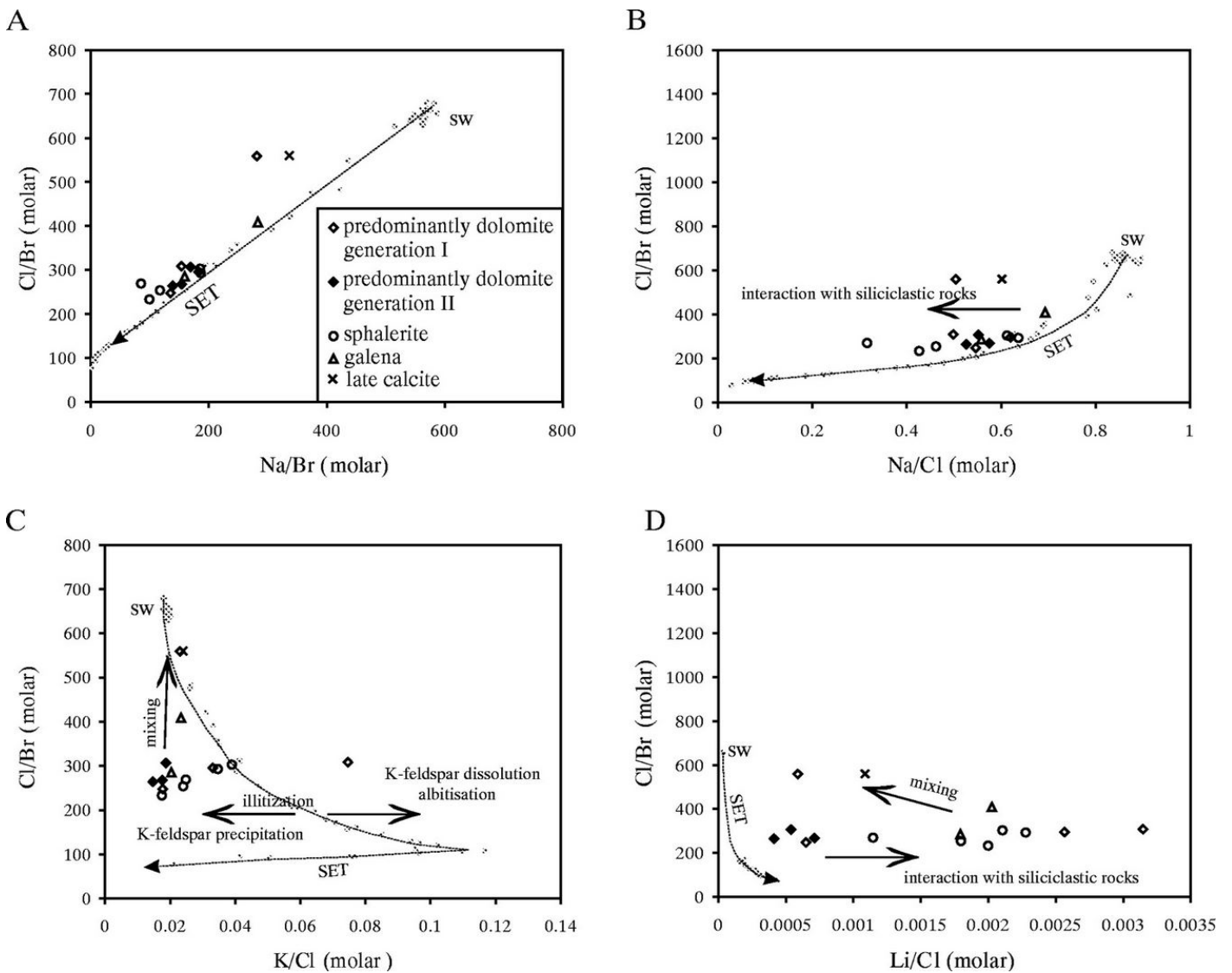


Figure 5: Covariance plots of crush-leach analysis results of inclusion fluids in different minerals (see legend). SET = Seawater Evaporation Trajectory (light gray data points and dotted line; data from McCaffrey et al., 1987) (Heijlen et al., 2003).

galena (G2), and late calcite (Mc2) (Figure 1). Comparison of Na/Br, Cl/Br, Na/Cl, K/Cl, and Li/Cl ratios of the fluids in the samples to that of seawater provide insight into the origin of the brines as well as the kind of fluid-rock interaction the fluids experienced before entrapment. Due to the small distribution coefficient of Br in halite (McAffrey et al., 1987), it is possible to see whether the fluids originated by the dissolution of evaporites or by residual brines from the evaporation of seawater. Brine that has developed its salinity from dissolving evaporates will have low Br values and thus elevated Na/Br, Cl/Br compared to seawater (molar Na/Br~540, molar Cl/Br~638, Heijlen et al., 2003). Residual brines from the evaporation of seawater will have high Br values and thus low Na/Br and Cl/Br ratios, and will follow the Seawater Evaporation Trajectory (SET, Figures 4A and B). Additionally, the sample fluids show lower Na/Br and Na/Cl ratios compared to seawater, suggesting interaction occurred with siliclastic rocks.

K-content in the fluids can often reflect processes such as illitization and albitization (decreasing K and increasing K, respectively). By evaluating Figure 5C, it is possible to see that the samples had a variety of K concentrations and suggests that both of these processes may have affected the mineralizing fluids. Further support that the fluid interacted with clay minerals is illustrated by evaluating the Li/Cl ratios (Figure 5D) which can be seen have an elevated Li/Cl ratio compared to evaporating seawater.

Conclusions

The results of these studies indicate that the system experienced episodic fluid introduction due to changing salinity and temperature values, as well as the presence of secondary inclusions of high-salinity, H₂O-NaCl-CaCl₂ nature in brecciated post-ore calcite. The fluids originated from the evaporation of seawater, and experienced siliclastic diagenesis seen by the variety of K and Li content. Heijlen et al. (2003) argue the faults in the system played a major role as a fluid conduit and in the evolution of the ore-bearing fluids. Kozłowski (1995) stated that saline formation waters mixed with ascending solutions (likely through the fault zones), and later mixed with meteoric wa-

ters due to a sharp decrease in salinity and temperature. For more information on genetic models, see the chapter on the geology of the Pomorzany and Olkusz mine by T. Solms (page 32).

References

- Heijlen, W., Muchez, P., Banks, D.A., Schneider, J., Kucha, H., and Keppens, E. (2003): Carbonate-Hosted Zn-Pb deposits in Upper Silesia, Poland: origin and evolution of mineralizing fluids and constraints on genetic models. *Economic Geology* 98, 911–932.
- Kozłowski, A. (1995): Origin of Zn-Pb ores in the Olkusz and Chrzanow districts: A model based on fluid inclusions. *Acta Geologica Polonica* 45, 83-141.
- McCaffrey, M.A., Lazar, B., and Holland, H.D. (1987): The evaporation path of seawater and the coprecipitation of Br and K with halite. *Journal of Sedimentary Petrology* 57, 928–937.

The Piast-Ziemowit hard coal mine, underground techniques

Farid Zabihian

- Hard coal deposits of Poland belong to Carboniferous age, originated in three basins: Upper Silesian Coal Basin (USCB), Lublin Coal Basin (LCB) and Lower Silesian Coal Basin (LSCB)
- Underground coal gasification (UCG) is significantly cost-saving and lessens environmental impacts by not requiring the coal to be mined in order to be gasified
- Wastes are divided into mining wastes and processing wastes and they can be recovered and used by different means.

Introduction

Poland is the second largest coal producer in Europe and 8th in the world and is also a main importer of other fossil fuels. In 2015, the total hard coal resources and reserves were 56,220 Mt and 21,107 Mt, respectively, and 51.2 Mt were consumed. Power generation from hard coal was about 80 TWh out of about 165 TWh total gross power generated (U.S. Energy Information Administration, 2016, Polish Geological Institute, 2015). At the end of 2016, as per the provided production data of all hard coal mines, total production was about 66 Mt, showing an increase of 2.17% in comparison to the previous year (Malon and Tymiński, n.d.). The statistics of resources and output during between 1989-2016 are shown in Figure 1.

Hard coal deposits are formed in the Carboniferous Euro-American coal region which is known by two

belts of coal basins in Europe. Paralic coal basins initiated near the sea in depressions along the front of the Variscan fold belt, and limnic basins, with coals that accumulated in closed basins. In Poland, coal deposits are of Carboniferous age and occur in three basins: the Upper Silesian Coal Basin (USCB) and Lublin Coal Basin (LCB, paralic type), and the Lower Silesian Coal Basin (LSCB), which is the limnic type, the latter comprises five deposits, which are now abandoned (Malon and Tymiński, n.d.).

Piast-Ziemowit hard coal mines

The Piast coal mine and the neighboring Ziemowit coal mine are two of the largest mines in the southern part of Poland, located 310 km southwest of the capital. Their total coal reserve is estimated to be about 283 Mt (Kompania Węglowa S.A., 2009).

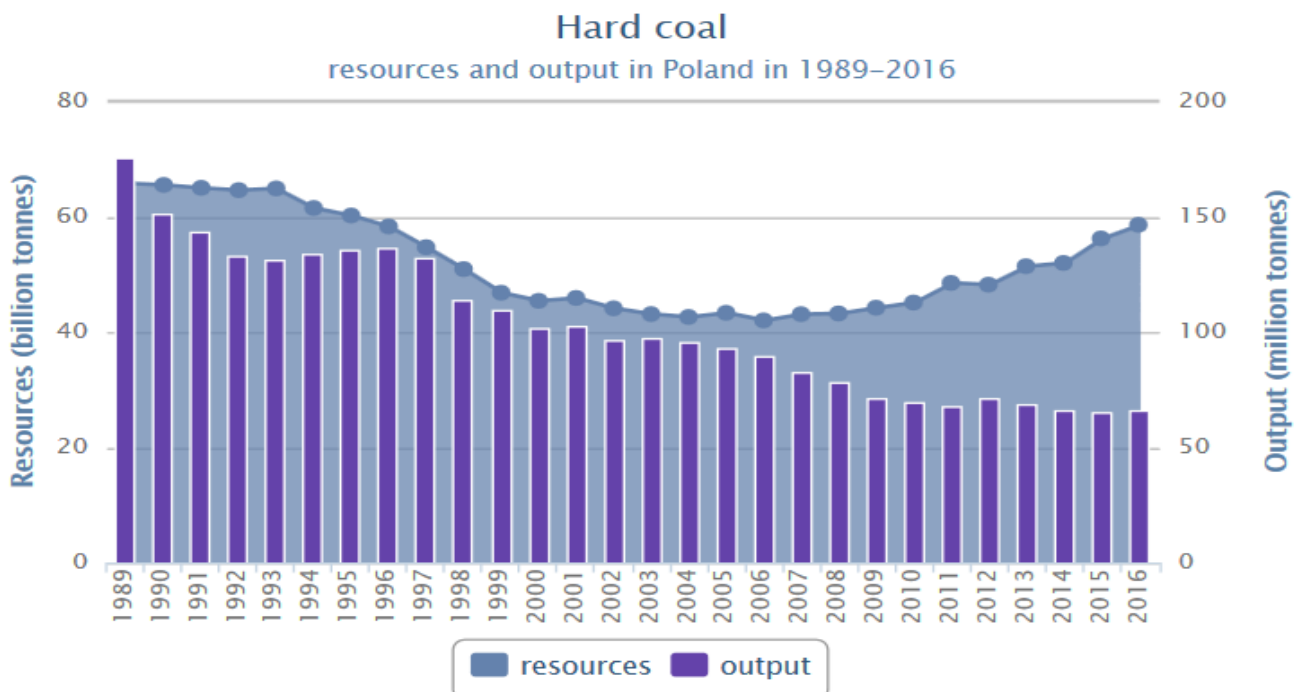


Figure 1: Changes in resources and production of hard coal in Poland from the years 1989-2016, from Malon and Tymiński (n.d.).

The USCB is the main coal basin in Poland. Except one large mine, all other hard coal mines of Poland are located in this basin. The USCB exists both in Czech Republic and Poland in its Polish part covers an area estimated to be about 5,600 km². At present forecasted economic resources of the USCB constitute about 80% of domestic resources of Poland. The stratigraphic cross-section of the USCB is shown in Figure 2 (Malon and Tyimiński, n.d.).

Mining techniques to utilize the coal extraction

Coal serves for energy production at relatively low cost. But, various technologies are required to reduce its negative impact on the environment and enhance its recovery. Some of these techniques are reviewed here:

Underground coal gasification (UCG): One of the technologies to enable the future utilization of coal for energy is underground coal gasification (UCG). It reduces the emissions of pollutants such as mercury, sulfur, and nitrous oxides. By injecting enriched air or

oxygen to the underground coal seam, the seam itself becomes the reactor, so that the gasification of the coal will be done underground instead of in a manufactured gasification vessel at the surface. This process is very cost-saving and reduces the environmental impacts by not requiring the coal to be mined in order to be gasified. However, there are some negative impacts as well.

One of the most important parameters which shall be taken into account for choosing suitable mines for this process is the natural water inflow, which causes a considerably greater impact on UCG than the bed moisture itself. There is a limit for existence of water in place and the excess water needs to be pumped out for production of usable low-calorific gas (Białecka, 2008).

Studies have shown the Ziemowit mine is one of the most appropriate choices with respect to the realization of UCG, considering all aspects including tectonics, methane hazards, seismic hazards, fire hazards, and rockburst hazards (Białecka, 2008).

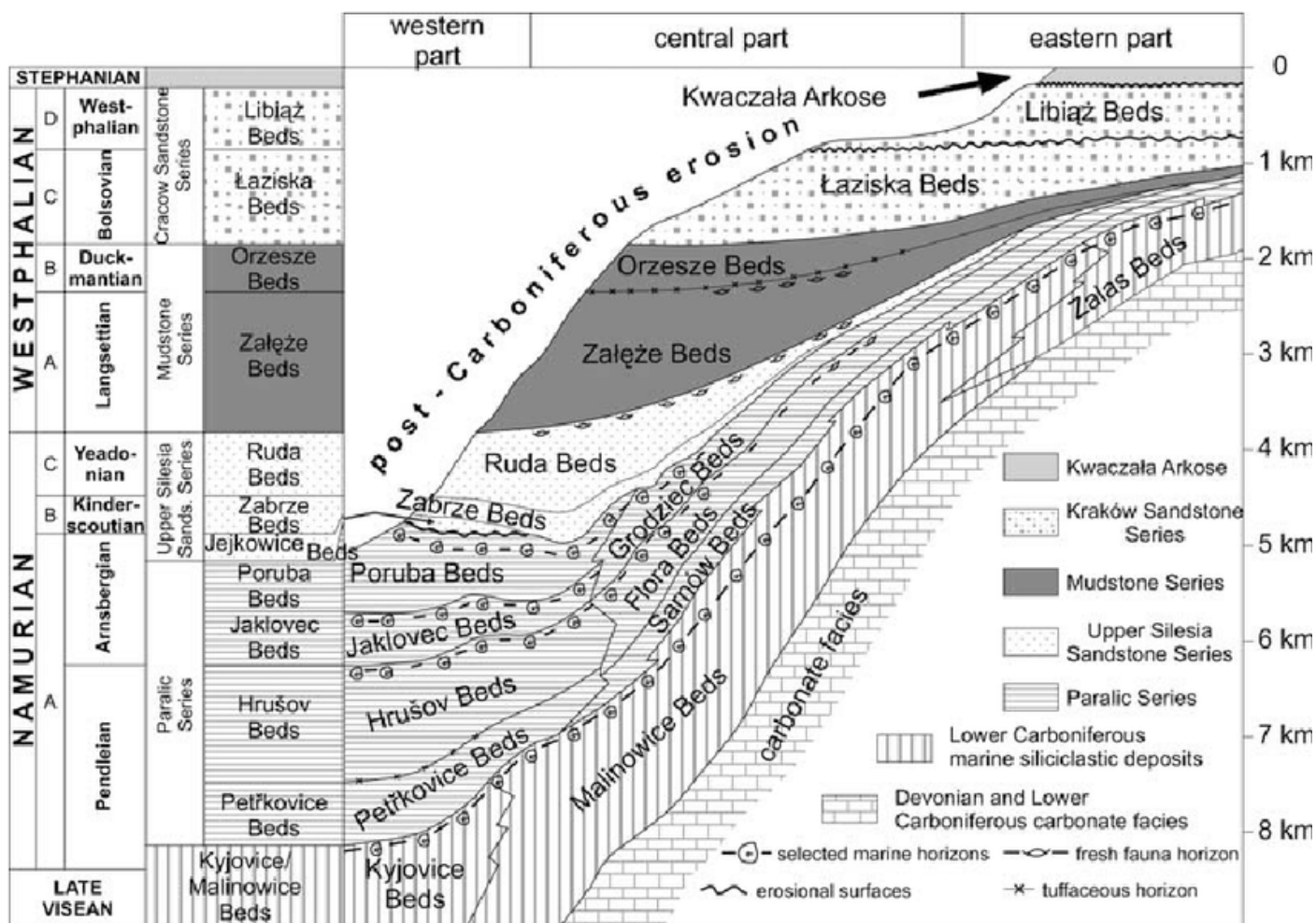


Figure 2: Stratigraphic cross-section through Upper Silesia Coal Basin infill, showing the age, reconstructed distribution and thickness of the main lithostratigraphical units, modified after Kotas (1994), from Doktor (2007).

Wastes: The mining process causes many wastes in the environment. Another technology to utilize the mining process is to reduce the amount of these wastes in different ways, for example, by using them in other industries.

Wastes from the mining and processing of hard coal come from barren sedimentary Carboniferous rocks, which are extracted along with hard coal seams. The waste is divided to mining waste and processing waste. The mining waste is produced by preparatory and productive mining works, with different quality parameters based on rock types and geological conditions of extracted deposits. The processing waste is produced by hard coal processing, depending on the type of processing equipment used and the applied technologies (Galos and Szlugaj, 2014).

The mentioned wastes - after recovery by variable methods - can be used in: engineering, hydrotechnical applications, road construction (including aggregate production), production of cement or building ceramics, recovery of coal, backfilling material, building ceramics, and cement clinker manufacture. Other applications include: coal recovery from coal wastes and granulated coal mud production (Galos and Szlugaj, 2014).

References

Białecka, B. (2008): Estimation of Coal Reserves for UCG in the Upper Silesian Coal Basin, Poland. *Natural Resources Research* 17, 21-28.

Doktor, M. (2007): Conditions of accumulation and sedimentary architecture of the upper Westphalian Cracow Sandstone Series (Upper Silesia Coal Basin, Poland). *Annales Societatis Geologorum Poloniae* 77, 219-268.

Galos, K. and Szlugaj, J. (2014): Management of hard coal mining and processing wastes in Poland. *Gospodarka Surowcami Mineralnymi – Mineral Resources Management* 30, 51-64.

Kompania Węglowa S.A. (2009), accessed 07.06.2018: Informacje ogólne o kopalni. <https://web.archive.org/web/20100527213918/http://www.kwsa.pl/22,zie,Odzia%C5%82%20KWK%20Ziemowit.html>.

Malon, A. and Tymiński, M. (n.d.), accessed 07.06.2018: http://geoportal.pgi.gov.pl/surowce/energetyczne/wegiel_kamienny.

Polish Geological Institute (2015), accessed 07.06.2018: <https://euracoal.eu/info/country-profiles/poland/>.

U.S. Energy Information Administration (2016), accessed 07.06.2018: www.eia.gov.

The Tarnowskie Góry mining museum

Cyrielle Bernard

- Tarnowskie Góry mine was exploited from 1526 to 1912 for lead and silver.
 - It is located in the Cracow-Silesian district, a highly deformed zone.
- Ore deposits are mainly Zn, Pb, and Ag in dolomites of Muschelkalk age.
 - The deposit is a MVT, hence many sulphides can be found.

Introduction

The name Tarnowskie Góry comes from „Tarnowice“ a village where high concentrations of lead and silver were historically found; and „Góry“ that means „mountains“, referring to the bumps around shafts dug for mining. Hence, Tarnowskie Góry has a long



Figure 1: An example of what can be seen by tourists in the Tarnowskie Góry mine (Historic Silver Mine, n.d.).

history of mining that began in 1526 when the Duke of Opole, John II, gave it the status of an independent mining town for lead, zinc, and silver. Some propose that the lead exported from the Tarnowskie Góry mine contributed to the development of international trade in Europe, when silver was sent to China to make coins. In the early 1700s, the mine was one of the first to use steam engines to extract lead and silver. Mining activity continued until resources were exhausted, in 1912. Today, a museum lets people know about mining exploitation, from pickaxe to steam engine, before entering the mine itself (Figure 1). It is currently partly flooded, but can be visited by foot and boat.

Geological setting

The mine of Tarnowskie Góry is located in the Cracow-Silesian district, south Poland (Fig. 2). This district is located at the junction of three main zones: a geosynclinal of Caledonian origin, the Variscan Upper Silesia Coal Basin, and the Carpathian foredeep of Cretaceous age (linked to the Alpine orogeny). Hence, it is a major boundary zone that underwent three intense deformation periods during the Caledonian, Variscan, and Alpine orogeneses. These deformations produced folds, faults and grabens repeatedly reacti-

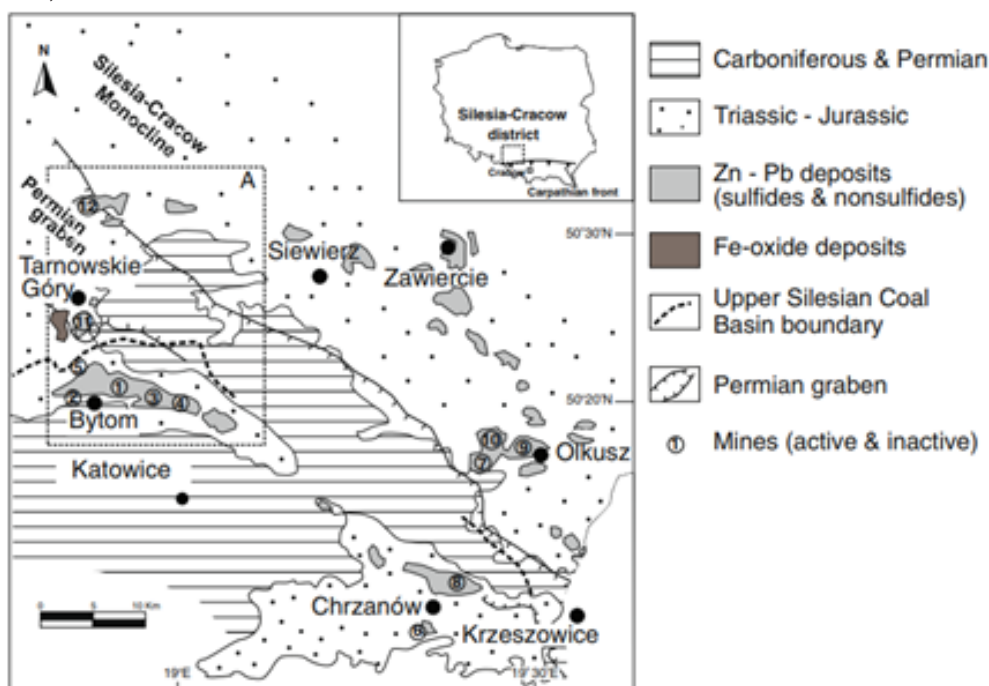


Figure 2: Schematic geological map of the Silesia-Cracow mining district. 1 Warynski, 2 Marchlewski, 3 Orzel Bialy, 4 Dabrowka, 5 Nowy Dwor, 6 Matyllda, 7 Boleslaw, 8 Trzebionka, 9 Olkusz, 10 Pomorzany, 11 Fryderyk, 12 Bibiela-Kalety. From Coppola et al. (2009).

vated through time. In these weak zones, ore minerals concentrate as replacement phases, cavity fillings, veins, and mineralized breccias. Ore deposits, mainly zinc (Zn), lead (Pb), and silver (Ag), are hosted in carbonates, mostly dolomites, of the Muschelkalk (235–245 Ma). These carbonates are part of a Mesozoic platform that recorded periods of marine transgression and regression from Triassic to Late Cretaceous. Today, they form a karstic landscape. Under the platform, the basement of Precambrian age is overlain by several kilometres of Palaeozoic metamorphosed sedimentary rocks.

Ore formation

Ore-bearing dolomite is first of diagenetic origin, but it seems that most of it also corresponds to a Mississippi-Valley-Type (MVT) origin. Diagenetic ore-bearing dolomites are generally fine-grained, while MVT ones are coarser-grained sulphides. To form MVT deposits, both marine fluids enriched in H_2S , and hydrothermal fluids of a different origin previously enriched in rare metals (usually lead and zinc) are required. The origin of these metals depends on the context. The marine fluids, highly saline and cold, infiltrate and circulate in the carbonate rocks of the platform, where basic hydrothermal fluids are already present. The mixing between the two fluids at different pH destabilizes metals originally dissolved, which locally deposits sulphides in high concentrations (see Figure 3).

In the Cracow-Silesian district, evidence tends to prove that the general paragenetic sequence was emplaced in a single short hydrothermal event. From oldest

to youngest minerals, are diagenetic dolomite, dolomite $[CaMg(CO_3)_2]$, MVT deposit sulphides such as pyrite (FeS_2), marcasite (FeS_2), sphalerite (ZnS), galena (PbS), and late-gangue minerals calcite ($CaCO_3$), barite ($BaSO_4$), chalcedony (SiO_2), and quartz (SiO_2). Accessory minerals are lead-arsenic complex sulphides such as jordanite $[Pb_{14}(As,Sb)_6S_{23}]$ and gratonite $[Pb_9As_4S_{15}]$. Silver (Ag), along with Cd, Ge, Ga, As, Tl, Sb and Ni usually occur as substitutions or microinclusions in sulphides.

References

Coppola, V., Boni, M., Gilg, H.A., and Strzelska-Smakowska, B. (2009): Nonsulfide zinc deposits in the Silesia-Cracow district, Southern Poland. *Mineralium Deposita* 44, 559–580.

De Vos, W., Batista, M.J., Demetriades, A., Duris, M., Lexa, J., Lis, J., Marsina, K., and O'Connor, P. (2005): Metallogenic mineral provinces and world class ore deposits in Europe. *Geochemical Atlas of Europe*, Part 1, 43–49.

Peter, J., Layton-Matthews, D., Gadd, M., Gill, S., Baker, S., Plett, S., and Paradis, S. (2015): Application of Visible-Near Infrared and Short Wave Infrared Spectroscopy to Sediment-hosted Zn-Pb Deposit Exploration in the Selwyn Basin, Yukon. *Targeted Geoscience Initiative* 4, 152–172.

Symons, D.T.A., Sangster, D.F., and Leach, D.L. (1995): A Tertiary age from paleomagnetism for mississippi valley-type zinc-lead mineralization in Upper Silesia, Poland. *Economic Geology* 90, 782–794.

Historic Silver Mine (n.d.), accessed 24.05.2018: <http://kopalniasrebra.pl/en/touring/touring-groups/>.

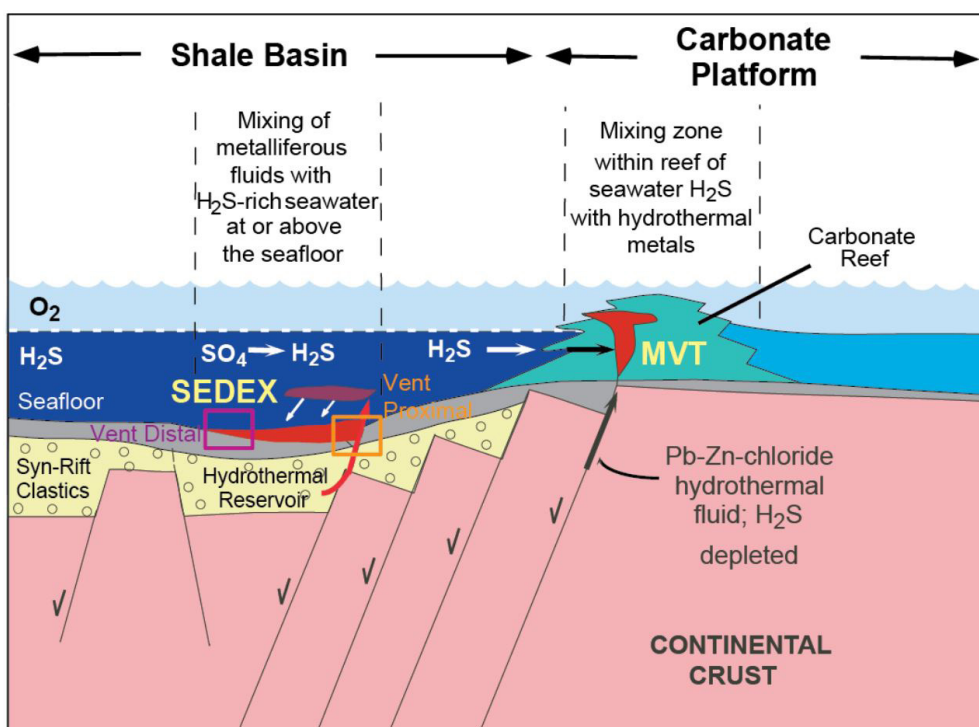


Figure 3: Formation of an MVT deposit, from Peter et al. (2015).



IUGS

www.stratigraphy.org

International Commission on Stratigraphy

v 2017/02



INTERNATIONAL CHRONOSTRATIGRAPHIC CHART

Phanerozoic				Eonothem / Eon				
Mesozoic		Cenozoic		Erathem / Era				
Cretaceous		Paleogene		System / Period				
				Series / Epoch				
				Stage / Age				
				GSSP				
				numerical age (Ma)				
Lower	Upper	Paleocene	Danian	Maastrichtian	Holocene	present		
					Pleistocene	0.0117		
					Pliocene	Zanclean	3.600	
						Messinian	5.333	
					Miocene	Tortonian	7.246	
						Serravallian	11.63	
						Langhian	13.82	
					Oligocene	Burdigalian	15.97	
						Aquitanian	20.44	
					Eocene	Chattian	23.03	
Rupelian	27.82							
Priabonian	33.9							
Bartonian	37.8							
Paleogene	Lutetian	41.2						
	Ypresian	47.8						
	Thanetian	56.0						
Cenozoic	Selandian	59.2						
	Danian	61.6						
Cretaceous	Upper	Paleocene	Danian	Maastrichtian	Holocene	0.0117		
						Pleistocene	Middle	0.126
							Calabrian	0.781
						Pliocene	Gelasian	1.80
							Placenzian	2.58
							Zanclean	3.600
						Miocene	Messinian	5.333
							Tortonian	7.246
							Serravallian	11.63
						Oligocene	Burdigalian	15.97
Aquitanian	20.44							
Eocene	Chattian	23.03						
	Rupelian	27.82						
	Priabonian	33.9						
	Bartonian	37.8						
Paleogene	Lutetian	41.2						
	Ypresian	47.8						
	Thanetian	56.0						
Cenozoic	Selandian	59.2						
	Danian	61.6						
Cretaceous	Upper	Paleocene	Danian	Maastrichtian	Holocene	0.0117		
						Pleistocene	Middle	0.126
							Calabrian	0.781
						Pliocene	Gelasian	1.80
							Placenzian	2.58
							Zanclean	3.600
						Miocene	Messinian	5.333
							Tortonian	7.246
							Serravallian	11.63
						Oligocene	Burdigalian	15.97
Aquitanian	20.44							
Eocene	Chattian	23.03						
	Rupelian	27.82						
	Priabonian	33.9						
	Bartonian	37.8						
Paleogene	Lutetian	41.2						
	Ypresian	47.8						
	Thanetian	56.0						
Cenozoic	Selandian	59.2						
	Danian	61.6						

Phanerozoic				Eonothem / Eon													
Paleozoic		Mesozoic		Erathem / Era													
Carboniferous		Triassic		System / Period													
				Series / Epoch													
				Stage / Age													
				GSSP													
				numerical age (Ma)													
Lower	Upper	Permian	Guadalupian	Artinskian	Kimmeridgian	~145.0											
						Lopingian	Wuchapingian	251.902 ±0.024									
							Changhsingian	254.14 ±0.07									
						Triassic	Induan	247.2									
							Olenekian	251.2									
							Anisian	~242									
						Mesozoic	Lower	Lopingian	Wuchapingian	Changhsingian	Kimmeridgian	~227					
												Triassic	Upper	Norian	Rhaetian	Toarcian	~208.5
																	Jurassic
												Jurassic	Middle	Aalenian	Bajocian	Callovian	
Upper	Oxfordian	Toarcian	Pliensbachian	182.7 ±0.7													
				Carnian	Ladinian	Anisian	Olenekian	163.5 ±1.0									
Carboniferous	Pennsylvanian	Upper	Kasimovian					Gzhelian	Kimmeridgian	152.1 ±0.9							
				Middle	Moscovian	Bashkirian	Serpukhovian			157.3 ±1.0							
										Lower	Viséan	Tournaisian	166.1 ±1.2				
Carboniferous	Mississippian	Lower	Viséan	Tournaisian	Kimmeridgian	168.3 ±1.3											
						Middle	Moscovian	Bashkirian	Serpukhovian	170.3 ±1.4							
										Upper	Kasimovian	Gzhelian	Kimmeridgian	174.1 ±1.0			
Carboniferous	Pennsylvanian	Upper	Kasimovian	Gzhelian	Kimmeridgian	182.7 ±0.7											
						Middle	Moscovian	Bashkirian	Serpukhovian	Tournaisian	190.8 ±1.0						
Lower	Viséan	Tournaisian	Kimmeridgian	Toarcian	199.3 ±0.3												
					Carboniferous	Mississippian	Lower	Viséan	Tournaisian	Kimmeridgian	201.3 ±0.2						
Middle	Moscovian	Bashkirian	Serpukhovian	Tournaisian							190.8 ±1.0						
											Upper	Kasimovian	Gzhelian	Kimmeridgian	182.7 ±0.7		
Carboniferous	Pennsylvanian	Upper	Kasimovian	Gzhelian	Kimmeridgian	163.5 ±1.0											
						Middle	Moscovian	Bashkirian	Serpukhovian	Tournaisian	166.1 ±1.2						
Lower	Viséan	Tournaisian	Kimmeridgian	Toarcian	168.3 ±1.3												
					Carboniferous	Mississippian	Lower	Viséan	Tournaisian	Kimmeridgian	170.3 ±1.4						
Middle	Moscovian	Bashkirian	Serpukhovian	Tournaisian							174.1 ±1.0						
											Upper	Kasimovian	Gzhelian	Kimmeridgian	182.7 ±0.7		
Carboniferous	Pennsylvanian	Upper	Kasimovian	Gzhelian	Kimmeridgian	190.8 ±1.0											
						Middle	Moscovian	Bashkirian	Serpukhovian	Tournaisian	199.3 ±0.3						
Lower	Viséan	Tournaisian	Kimmeridgian	Toarcian	201.3 ±0.2												
					Carboniferous	Mississippian	Lower	Viséan	Tournaisian	Kimmeridgian	251.902 ±0.024						
Middle	Moscovian	Bashkirian	Serpukhovian	Tournaisian							247.2						
											Upper	Kasimovian	Gzhelian	Kimmeridgian	~242		
Carboniferous	Pennsylvanian	Upper	Kasimovian	Gzhelian	Kimmeridgian	~237											
						Middle	Moscovian	Bashkirian	Serpukhovian	Tournaisian	Kimmeridgian	~227					
Lower	Viséan	Tournaisian	Kimmeridgian	Toarcian	Pliensbachian							~208.5					
						Carboniferous	Mississippian	Lower	Viséan	Tournaisian	Kimmeridgian	199.3 ±0.3					
Middle	Moscovian	Bashkirian	Serpukhovian	Tournaisian	190.8 ±1.0												
					Upper							Kasimovian	Gzhelian	Kimmeridgian	182.7 ±0.7		
Carboniferous	Pennsylvanian	Upper	Kasimovian	Gzhelian		Kimmeridgian	163.5 ±1.0										
					Middle		Moscovian	Bashkirian	Serpukhovian	Tournaisian	Kimmeridgian	166.1 ±1.2					
Lower	Viséan	Tournaisian	Kimmeridgian	Toarcian		Pliensbachian						168.3 ±1.3					
					Carboniferous		Mississippian	Lower	Viséan	Tournaisian	Kimmeridgian	170.3 ±1.4					
Middle	Moscovian	Bashkirian	Serpukhovian	Tournaisian		174.1 ±1.0											
						Upper						Kasimovian	Gzhelian	Kimmeridgian	182.7 ±0.7		
Carboniferous	Pennsylvanian	Upper	Kasimovian	Gzhelian	Kimmeridgian		190.8 ±1.0										
						Middle	Moscovian	Bashkirian	Serpukhovian	Tournaisian	Kimmeridgian	199.3 ±0.3					
Lower	Viséan	Tournaisian	Kimmeridgian	Toarcian	Pliensbachian							201.3 ±0.2					
						Carboniferous	Mississippian	Lower	Viséan	Tournaisian	Kimmeridgian	251.902 ±0.024					
Middle	Moscovian	Bashkirian	Serpukhovian	Tournaisian	247.2												
					Upper							Kasimovian	Gzhelian	Kimmeridgian	~242		
Carboniferous	Pennsylvanian	Upper	Kasimovian	Gzhelian		Kimmeridgian	~237										
					Middle		Moscovian	Bashkirian	Serpukhovian	Tournaisian	Kimmeridgian	~227					
Lower	Viséan	Tournaisian	Kimmeridgian	Toarcian		Pliensbachian						~208.5					
					Carboniferous		Mississippian	Lower	Viséan	Tournaisian	Kimmeridgian	199.3 ±0.3					
Middle	Moscovian	Bashkirian	Serpukhovian	Tournaisian		190.8 ±1.0											
						Upper						Kasimovian	Gzhelian	Kimmeridgian	182.7 ±0.7		
Carboniferous	Pennsylvanian	Upper	Kasimovian	Gzhelian	Kimmeridgian		163.5 ±1.0										
						Middle	Moscovian	Bashkirian	Serpukhovian	Tournaisian	Kimmeridgian	166.1 ±1.2					
Lower	Viséan	Tournaisian	Kimmeridgian	Toarcian	Pliensbachian							168.3 ±1.3					
						Carboniferous	Mississippian	Lower	Viséan	Tournaisian	Kimmeridgian	170.3 ±1.4					
Middle	Moscovian	Bashkirian	Serpukhovian	Tournaisian	174.1 ±1.0												
					Upper							Kasimovian	Gzhelian	Kimmeridgian	182.7 ±0.7		
Carboniferous	Pennsylvanian	Upper	Kasimovian	Gzhelian		Kimmeridgian	190.8 ±1.0										
					Middle		Moscovian	Bashkirian	Serpukhovian	Tournaisian	Kimmeridgian	199.3 ±0.3					
Lower	Viséan	Tournaisian	Kimmeridgian	Toarcian		Pliensbachian						201.3 ±0.2					
					Carboniferous		Mississippian	Lower	Viséan	Tournaisian	Kimmeridgian	251.902 ±0.024					
Middle	Moscovian	Bashkirian	Serpukhovian	Tournaisian		247.2											
						Upper						Kasimovian	Gzhelian	Kimmeridgian	~242		
Carboniferous	Pennsylvanian	Upper	Kasimovian	Gzhelian	Kimmeridgian		~237										
						Middle	Moscovian	Bashkirian	Serpukhovian	Tournaisian	Kimmeridgian	~227					
Lower	Viséan	Tournaisian	Kimmeridgian	Toarcian	Pliensbachian							~208.5					
						Carboniferous	Mississippian	Lower	Viséan	Tournaisian	Kimmeridgian	199.3 ±0.3					
Middle	Moscovian	Bashkirian	Serpukhovian	Tournaisian	190.8 ±1.0												
					Upper							Kasimovian	Gzhelian	Kimmeridgian	182.7 ±0.7		
Carboniferous	Pennsylvanian	Upper	Kasimovian	Gzhelian		Kimmeridgian	163.5 ±1.0										
					Middle		Moscovian	Bashkirian	Serpukhovian	Tournaisian	Kimmeridgian	166.1 ±1.2					
Lower	Viséan	Tournaisian	Kimmeridgian	Toarcian		Pliensbachian						168.3 ±1.3					
					Carboniferous		Mississippian	Lower	Viséan	Tournaisian	Kimmeridgian	170.3 ±1.4					
Middle	Moscovian	Bashkirian	Serpukhovian	Tournaisian		174.1 ±1.0											
						Upper						Kasimovian	Gzhelian	Kimmeridgian	182.7 ±0.7		
Carboniferous	Pennsylvanian	Upper	Kasimovian	Gzhelian	Kimmeridgian		190.8 ±1.0										
						Middle	Moscovian	Bashkirian	Serpukhovian	Tournaisian	Kimmeridgian	199.3 ±0.3					
Lower	Viséan	Tournaisian	Kimmeridgian	Toarcian	Pliensbachian							201.3 ±0.2					
						Carboniferous	Mississippian	Lower	Viséan	Tournaisian	Kimmeridgian	251.902 ±0.024					
Middle	Moscovian	Bashkirian	Serpukhovian	Tournaisian	247.2												
					Upper							Kasimovian	Gzhelian	Kimmeridgian	~242		
Carboniferous	Pennsylvanian	Upper	Kasimovian	Gzhelian		Kimmeridgian	~237										
					Middle		Moscovian	Bashkirian	Serpukhovian	Tournaisian	Kimmeridgian	~227					
Lower	Viséan	Tournaisian	Kimmeridgian	Toarcian		Pliensbachian						~208.5					
					Carboniferous		Mississippian	Lower	Viséan	Tournaisian	Kimmeridgian	199.3 ±0.3					
Middle	Moscovian	Bashkirian	Serpukhovian	Tournaisian		190.8 ±1.0											
						Upper						Kasimovian	Gzhelian	Kimmeridgian	182.7 ±0.7		
Carboniferous	Pennsylvanian	Upper	Kasimovian	Gzhelian	Kimmeridgian		163.5 ±1.0										
						Middle	Moscovian	Bashkirian	Serpukhovian	Tournaisian	Kimmeridgian	166.1 ±1.2					
Lower	Viséan	Tournaisian	Kimmeridgian	Toarcian	Pliensbachian							168.3 ±1.3					
						Carboniferous	Mississippian	Lower	Viséan	Tournaisian	Kimmeridgian	170.3 ±1.4					
Middle	Moscovian	Bashkirian	Serpukhovian	Tournaisian	174.1 ±1.0												
					Upper							Kasimovian	Gzhelian	Kimmeridgian	182.7 ±0.7		
Carboniferous	Pennsylvanian	Upper	Kasimovian	Gzhelian		Kimmeridgian	190.8 ±1.0										
					Middle		Moscovian	Bashkirian	Serpukhovian	Tournaisian	Kimmeridgian	199.3 ±0.3					
Lower	Viséan	Tournaisian	Kimmeridgian	Toarcian		Pliensbachian						201.3 ±0.2					
					Carboniferous		Mississippian	Lower	Viséan	Tournaisian	Kimmeridgian	251.902 ±0.024					
Middle	Moscovian	Bashkirian	Serpukhovian	Tournaisian		247.2											
						Upper						Kasimovian	Gzhelian	Kimmeridgian	~242		
Carboniferous	Pennsylvanian	Upper	Kasimovian	Gzhelian	Kimmeridgian		~237										
						Middle	Moscovian	Bashkirian	Serpukhovian	Tournaisian	Kimmeridgian	~227					
Lower	Viséan	Tournaisian	Kimmeridgian	Toarcian	Pliensbachian							~208.5					
						Carboniferous	Mississippian	Lower	Viséan	Tournaisian	Kimmeridgian	199.3 ±0.3					
Middle	Moscovian	Bashkirian	Serpukhovian	Tournaisian	190.8 ±1.0												
					Upper							Kasimovian	Gzhelian				